MASS TRANSPORT AND CHEMICAL KINETICS OF PLATELET ADHESION TO BIOMATERIALS

MASS TRANSPORT AND CHEMICAL KINETICS OF PLATELET ADHESION TO BIOMATERIALS

by

James M. Brophy

A Project Report

Submitted to the Faculty of Graduate Studies

in Partial Fulfilment of the Requirements

for the Degree

Master of Engineering

McMaster University

September 1974

Master of Engineering (1974) McMaster University
(Chemical Engineering) Hamilton, Ontario.

Title: Mass Transport and Chemical Kinetics of Platelet Adhesion to Biomaterials

Author: James M. Brophy, B.Eng. (McGill University)

Supervisors: Dr. J. L. Brash and Dr. I. A. Feuerstein

Number of Pages: x, 107.

Scope and Contents:

The operating procedure for a Couette flow apparatus capable of evaluating the thromboresistance (by examination of platelet adhesion) of materials was standardized. It was established that operating at room temperature instead of at the normal physiological temperature, 37°C, did not affect platelet adhesion and that a continued exposure to a shear rate of 19 sec^{-1} for 40 minutes did not damage the platelets. The radioisotope evaluation technique gave consistent results with the direct counting method.

Platelet diffusivity in the presence of red cells was found to be one or two orders of magnitude greater than the one predicted by Brownian motion and to be dependent on shear rate and hematocrit.

A theoretical model for platelet adhesion was developed for the diffusion limited case and described the experimental data for collagen coated glass.

Glass, polystyrene, sulphonated polystyrene and polyurethane reached equilibrium values of platelet adhesion after 2-10 minutes. The equilbrium values of these surfaces were not distinguishable. Albumin coated glass reached an equilibrium

value in less than 2 minutes that was substantially lower than the other surfaces investigated. Platelet adhesion to collagen, as predicted by the diffusional model, continuod to increase with time.

ACKNOWLEDGEMENTS

I am very grateful to all the people who have contributed to this research.

Myron Kulczycky provided excellent technical assistance throughout my experimental work and I sincerely thank him.

I thank many stimulating conversations with D. J. Allen for increasing my understanding and appreciation of the field of biomedical engineering.

I would like to thank Dr. J. Brash and Dr. I. Feuerstein for supervising this research. Their careful reading of this thesis and helpful comments were appreciated.

I am grateful to BettyAnne Bedell for her patient and excellent typing of this manuscript.

TABLE OF CONTENTS

NOMENCLATURE

t	time
D_B	Brownian diffusion coefficient
D_p	platelet diffusivity
H	hematocrit
γ	shear rate
β	power law diffusivity exponent for hematocrit
n	power law diffusivity exponent for shear rate
C_o	bulk platelet concentration
K_B	Boltzman's constant
r	radial co-ordinate
f	fractional surface area not yet covered by platelets
T_a	Taylor number
Re	Reynolds number $\frac{\rho Ud}{\mu}$
Re_p	particle Reynolds number $\frac{\rho Udp}{\mu}$
ρ	fluid density
μ	fluid viscosity
R_o	tube radius diameter
ℓ	characteristic length
dp	particle diameter
d	width of annulus
U_i	peripheral velocity of inner cylinder
R_1	radius of inner cylinder
ν	kinematic viscosity
K	apparent wall adhesion constant
S	platelet surface density

J	platelet flux
S_p	equilibrium platelet density
$\dot{\gamma}$	shear rate
T	temperature
b	particle radius
V_θ	velocity component in the θ direction
Ω	speed of rotating inner cylinder

LIST OF TABLES

LIST OF FIGURES

CHAPTER 1

INTRODUCTION

Tens of thousands of people are benefitting from surgical implants of many types. Many heart valves and heart pacemakers are implanted each year. Artificial kidneys, although external to the body, may be considered to act as implants since blood flows through these as an extension of the circulatory system.

The complications involved with these implants are enormous and largely due to the problem of blood compatibility. Platelet adhesion followed by thrombus formation and thromboembolism is one of the most serious problems of blood compatibility and gives rise to serious and often fatal complications with many vascular implants. Anticoagulation treatment does not eliminate the cellular interactions of blood with artificial surfaces and is often responsible for hemorrhagic disorders. Other immediate and drastic disturbances that arise from blood/artificial surface incompatibility are blood coagulation, alteration of blood proteins and enzymes, lysis of red blood cells and alteration of the phagocytic properties of white blood cells.

The urgency of finding biomaterials with appropriate blood compatibility properties is evident if continued progress is to be made in the present field of vascular implants and

future field of artificial organs.

The overall aim of this project was to develop a controlled flow apparatus capable of evaluating the thrombo-resistance of biomaterials. The concepts of fluid mechanics, mass transfer and chemical kinetics must be considered in the design, operation and interpretation of results of these experiments. Preliminary evaluation of platelet adhesion to materials was commenced after establishing the reliability of the experimental design. The experimental equipment was designed to perform under well defined Couette flow. A radioisotope evaluation technique was employed to determine the number of adhering platelets.

It was also hoped that the application of chemical engineering principles would assist in elucidating the mechanism of platelet adhesion.

CHAPTER 2

LITERATURE REVIEW

2.1 Physiology

2.1.1 Fluid Mechanics and Composition of Blood

For reasons that will become clear as we proceed, it is necessary to be familiar with the constituents of blood, their fluid mechanical properties and their interactions with each other and bounding surfaces in order to fully understand the phenomena of platelet adhesion.

Blood, a suspension of cellular materials, is composed of erythrocytes (red cells), leukocytes (white cells), and thrombocytes (platelets). The per cent volume of red cells in blood is usually referred to as the hematocrit and is easily determined by centrifuging the blood. This produces a straw coloured supernatant and sedimented red blood cells. The normal hematocrit in man is approximately 45% and may be taken as an indication of the total cell concentration since 99% by volume of the disperse phase in blood consists of erythrocytes. The normal white cell concentration is 1/600th the approximate concentration of erythrocytes, $5.0 \times 10^6/mm^3$. The remaining cellular component platelets, number from 250,000 - 500,000/mm^3 and comprise .25% of the volume fraction in whole blood. The three types of cells are all shaped as ellipsoids with diameters of the order of 8, 12 and 1 micron for red cells, white cells and platelets respectively. White cells and

platelets with their relatively small number and volume of cells compared to erythrocytes exert negligible effects on the fluid properties of blood. However it is suspected that the motion of erythrocytes will substantially influence the flow behaviour of platelets (1-6).

The suspending fluid of blood is known as plasma. Plasma has the following approximate composition

90%	H_2O
7%	Proteins
1%	Organics (Other)
1%	Inorganics

Normal human plasma has a viscosity of approximately 1.2 centipoise at 37°C and may be considered as a Newtonian fluid (7).

The main plasma proteins are albumin, fibrinogen, globulins and lipoproteins. These proteins maintain osmotic pressure, serve variously to prevent diseases, regulate the hemostasis of blood, and also function as buffers to assist in controlling the blood pH.

Among the cations and anions existing in blood are Na^+, K^+, Cl^-, Ca^{++}, HCO_3^-, and $PO_4^{\equiv}$.

An important macroscopic fluid property of blood is viscosity. The relative viscosity of blood (viscosity of suspension/viscosity of suspending phase) is 3-5 for a normal hematocrit of 40 - 50% and a shear rate of approximately 100/ sec^{-1} (1). This relative viscosity is much lower than that for a suspension with a comparable concentration of rigid

spherical particles (1,8). The shape and deformability of red blood cells are important reasons for the low relative viscosity. For example, the altered shape and deformability accompanying sickle cell disease or aldehyde treatment produce higher relative viscosities (1).

At low shear rates blood behaves as a non-Newtonian fluid with a finite yield stress of approximately 0.01 dynes/cm^2 (9,10). More specifically blood is referred to as a pseudo-plastic as the apparent viscosity decreases with increasing shear rates (9, 11).

The non-Newtonian behaviour of blood is strongly influenced by hematocrit and red cell aggregation or rouleaux formation. The apparent viscosity of blood increases in a non-linear fashion with increasing hematocrit and this relation is shear rate dependent (3). Red cell suspensions in saline, without fibrinogen to induce aggregation, exhibit no yield stress and lower apparent viscosities than normal blood (7).

The above bulk rheological properties are important when attempting to solve the fluid mechanical equations of motion. However as we are interested in studying the process of platelet adhesion which occurs at a cellular level, the micro-rheological properties of blood must be considered in addition to the macrorheological properties discussed above.

The deformability of red blood cells must be acknowledged to accurately describe their flow properties. Goldsmith (2) has shown that red cells, in dilute suspensions, rotate and that the orientation of their major axis with the direction of flow

increases with increasing shear rate. This observation is consistent with the theory of deformable liquid drops. On the other hand, for rigid spheres the orientation distribution should be independent of shear rate.

In slow viscous flow ($Re_p < 10^{-6}$) with dilute red cell concentrations, a finite radial migration velocity toward the centerline is introduced due to a perturbation which results from the deformability of the red cell (2). At high Re numbers, the lateral migration is due to fluid inertial forces (12). Rigid spheres undergo lateral migration only at high Re numbers and an equilibrium is reached between migration from the wall and from the centerline (12).

This radial migration in blood flow results in a cell free zone at the bounding surface. This 'plasmatic zone' or skimming layer varies along the length of the tube (2) but in blood with a normal hematocrit is not expected to be thicker than the radius of a red blood cell (4 μ) (13). The thinness of this zone is due to the enormous number of particle collisions that occur at concentrations exceeding 5% (14). Bugliarello (15) has suggested that red cells penetrate this cell free layer due to the continuous interactions within blood at a rate that increases linearly with Re number and shear rate (4).

Goldsmith (2) has found dispersion coefficients of 3×10^{-8} cm^2/sec in bulk flow and 1.5×10^{-7} cm^2/sec in the vicinity of the wall ($R = 0.7\ Ro$). This means increasing dispersion coefficients are found in regions of increasing shear rate. These dispersion coefficients are 10-100 times larger

than the diffusion coefficients predicted by Brownian motion and are a result of the continuous sideways fluctuations of erythrocytes during flow (2).

The radial motions of red cells caused by cell-cell interactions will lead to a convective dispersion of dissolved substances such as proteins and platelets. The radial displacement of particles has been found to be a function of particle size in a manner analogous to Brownian motion (2). Goldsmith (2) has observed that 2 μ latex particles, the same size as platelets, in a 44% ghost (i.e., the hemoglobin has been removed from the red cells) cell suspension undergo radial displacements of 15 μ, 8 times their own diameter and double the mean free path of red blood cells. Therefore, it is expected that platelets will have a much greater collision rate with a bounding surface than red cells.

Keller (4) has further demonstrated semi-theoretically (but not rigourously) that rotation of red cells will, by means of stirring small volumes of suspending fluid, serve to augment particle diffusion. The resulting increase in diffusion is analogous to the increase in diffusion coefficients that arises when Re numbers are high enough to produce turbulent eddies. Following an analysis similar to Prandtl mixing length, Keller reaches the following formula for an isolated spherical red blood cell

$$D_p = 0.18\, a^2 \frac{du}{dy} \qquad (2.1)$$

where D_p - platelet diffusion coefficient augmented by particle rotation.

a - influence of rotation field (Approximately equal to radius of a red blood cell).

$\frac{du}{dy}$ - shear rate

At a shear rate of 100 sec^{-1}, D_p is approximately 3×10^{-6} cm^2/sec which again is large compared to the Brownian diffusion coefficients for large protein molecules or cells such as platelets. Molecules with a molecular weight less than the proteins are unlikely to experience an increase in diffusion due to the motions of red blood cells.

Keller (4) further found that increasing hematocrit at low Re numbers caused the number of cells penetrating the plasmatic or skimming layer to increase leading to a greater collision frequency with the wall.

Keller's hypothesis of secondary flows being associated with the rotational motion of red cells seems to be in some question as the cells in a 50% ghost suspension no longer undergo rotation (1). However other red cell motions may account for the augmented platelet diffusivities that have been experimentally observed (2, 16-19).

Bernstein et al. (5) and Blachshear et al. (6) have proposed a linear dependence for platelet diffusion on shear rate due to the augmented mass convection associated with red blood cell motions induced by fluid shear.

From the above, it is evident that the experimental equipment must be designed with well defined fluid flow conditions to elucidate the phenomena of platelet adhesion.

2.1.2 Platelet Functions and Definitions

Platelets have three prime functions. They are responsible for the formation of a hemostatic plug, acceleration of the coagulation process and support the endothdial cells of the vascular bed (20).

Before we discuss platelet functions and interactions with plasma proteins and boundary surfaces it is necessary to define some terminology. The literature on platelet accumulation to foreign surfaces or subendothelial structures has referred to this phenomena as adhesion, aggregation, agglutination, cohesion and agglomeration.

The following definitions are made to clarify the situation.

ADHESION: The fixation of single platelets on a surface to produce a partially complete or a complete monolayer.

COHESION: The additional adhesion of single platelets to platelets already adhering to the surface.

AGGREGATION: The interaction between platelets to produce a clump of platelets prior to adhesion.

THROMBI: Following Baumgarthor's (25, 26) definition platelet cohesion resulting in a layer exceeding 5 μ in height will be termed a thrombus. Thrombi occasionally have fibrin as well as platelets as a constituent (24).

The terms agglutination and agglomeration will not be employed here. Agglutination refers to platelet aggregation which is stimulated by antibodies.

Another term that is commonly used in accessing platelet/artificial surface interactions is thromboresistance. This is a relative concept since all artifical surfaces, to a greater or lesser effect, promote thrombus formation. The only true thromboresistant surface is the endothelial lining of blood vessels.

The first two properties of platelets mentioned above are of interest here. The hemostatic plug formed by vascular damage is similar to the thrombus generated on artifical surfaces in that the adhesion of platelets is the first microscopically identifiable phenomena (21). Platelets also play an important role in blood coagulation.

Blood coagulation is broadly classified into two distinct mechanisms known as the "intrinsic" and "extrinsic" systems (20, 27, 28). The "extrinsic" clotting mechanism is characterized by the release of tissue thromboplastin from damaged cells which catalyses the cascade reactions leading to coagulation. The "intrinsic" mechanism is initiated by components normally found in blood and platelet lipoproteins interact with plasma proteins to activate prothrombin to thrombin (20). The platelet lipoprotein responsible for this conversion is called platelet factor III (20). As indicated in Figure 1, it is unlikely that these two systems are completely independent. It appears that coagulation initiated by the extrinsic system will require thrombin that is formed intrinsically to assure the maintenance of a platelet plug (28).

MASS TRANSFER IN BIOLOGICAL SYSTEMS

PR

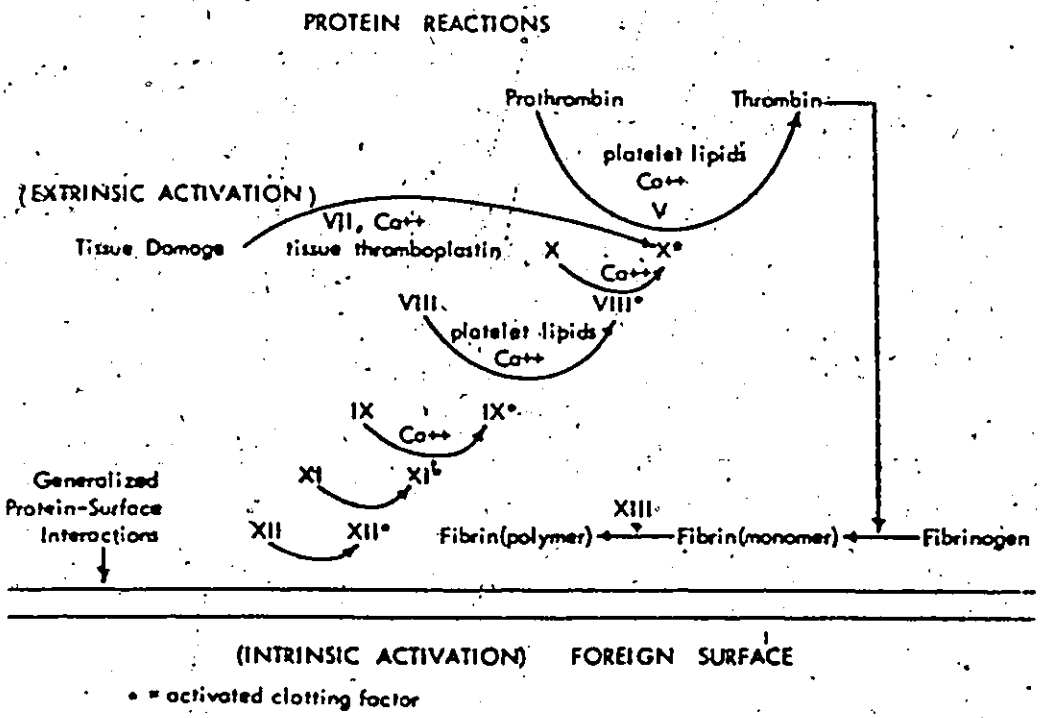

Fig. 1. Protein and cellular reactions in thrombogenesis. (From 29)

It is clear that platelets accelerate the clotting mechanism and that activation of factors VIII and V occur at the platelet membranes. It has been suggested that platelet factor III is a surface catalytic agent stimulated by the adhesion of platelets to surfaces (30).

Not only do platelets exert an influence on plasma proteins but the proteins also affect the function of platelets. From the cascade reaction we see that thrombin is produced by

both clotting mechanisms. Thrombin is known to cause pig platelets to aggregate (31) and further to cause the release of adenosine diphosphate (ADP) (32), serotonin and (33) degradation of ATP to ADP (28) (both known activators of platelet aggregation (34, 35). Fibrin, which is also formed in the clotting mechanism, may form a fibrous network on surfaces capable of entrapping red cells and platelets (20).

At the same time that the cascade reactions are occurring, heterogeneous protein-surface reactions are also believed to occur in advance of platelet adhesion (21, 22, 28). Among the surface active proteins believed to be adsorbed is fibrinogen (28). George (23) has claimed that fibrinogen, Ca^{++} and Mg^{++} are required for the adhesion of either unwashed or washed platelets. Other authors (36) have found fibrinogen to enhance the spreading of platelets on glass.

In our experiments, platelet adhesion occurred without the presence of free fibrinogen in the suspending medium. Furthermore the platelets adherent to collagen coated glass spread normally and developed psuedopods. This behaviour may be seen in the electron micrographs on pages 55, 56. Baumgartner (25) has found platelet adhesion without fibrin deposition for unaltered flow of 10-20 minutes through rabbit aortas denuded of endothelium.

From this it would appear that the platelet function of adhesion is not inhibited by the experimental suspending medium.

2.2 Biomaterials

The term biomaterials will cover all materials that are used in contact with mammalian blood and tissue. It includes biopolymers as well as materials made from naturally occuring protein.

We do not have to worry about protein adsorption triggering the intrinsic clotting mechanism and blood compatibility will refer solely to the cellular interactions between blood and the biomaterial beginning with platelet adhesion and culminating with thrombus formation.

The most difficult problem facing the use of biomaterials is blood compatibility. The biomaterial must also avoid the major problems of protein denaturation and red cell hemolysis. In addition, the characteristics of not being toxic, antigenic, carcinogenic and affected by sterilization are important.

Several criteria have been postulated to facilitate selection of blood compatible materials. These criteria will be briefly reviewed here and utilized, in a later section, to assist in the choice of materials to be examined.

In 1931, Lambert (37) found that coating glass with paraffin produced longer clotting times compared to untreated glass and consequently formulated the generalization that increased clotting times could be attained with hydrophobic materials. This generalization was the first attempt to characterize the properties of materials that do not initiate coagulation or thrombus formation.

However recent experiments have shown hydrophilic materials to be as effective as paraffin as a coating for glass (38).

Moreover, the intimina itself, which is thrombogenic, has been found to be hydrophilic (39). One is lead to conclude that surface wettability is not a decisive criterion for accessing blood compatibility.

Another early approach to the problem of biocompatibility was to complex heparin on the polymer surface (38). Heparin, a natural anticoagulent existing in the blood stream (40), has a molecular weight of approximately 16,000 and is obtained from beef lung or hog intestinal mucosa. A sodium salt is produced commercially and is commonly used to heparinize a material.

A third principle is to examine the electrical charge at the surface of the material. Since the natural lining of blood vessels and platelets are negatively charged, it has been suggested (38) that any artifical surface in contact with flowing blood should have a negative surface charge or at least be capable of permitting the development of a negative charge in situ. That an anionic surface enhances the performance of biomaterials is open to question as contradictory results may be found in a literature review by Leninger (38). Weiss (41), for example, has taken a theoretical approach to demonstrate that a repulsion due to like charges is not a sufficient barrier to platelet adhesion. It has also been reported (28, 42) that it is not the net charge that is important but instead the charge distribution.

The concept of enhanced blood compatibility due to a negative surface charge stimulated the initial research into

electrets. Electrets, insulators with internal electrical polarization, are found to favour increased clotting times, irregardless of surface charge (43). A possible explanation of the conflicting results regarding surface charge is that a protein layer may be adsorbed in a way not directly correlated with the electrical charge of the surface (44).

Another approach to the problem of blood-compatibility has been the investigation of inert surfaces. Although no surfaces have been found which are completely inert to blood, this group does differ from the ones previously mentioned in that they contain no highly negative groups or imposed electrical charges. Levowitz et al. (45) found little thrombus formation after one week of implantation of hydrogels of hydroxyethyl-methacrylate in dogs. Other materials that have shown good resistance to thrombus formation are hydrophilic methacrylates (46), and polyether urethane elastomers on methylene glycol or polypropylene glycol (47, 48).

Lyman et al. (49) have also studied inert surfaces in the form of uncharged hydrophobic polymers. They attempted to characterize blood clotting times as a function of the chemical nature and surface free energy of the polymer. These two parameters are important if one accepts the hypothesis that the surface free energy of a material is sufficient to induce coagulation in the blood/polymer system and that the chemical nature of the surface will affect coagulation through intermediary substances that are adsorbed. The authors approximated the surface free energy by the critical surface tension and found this to be inversely proportional to blood coagulation times.

Following this introductory work, Lyman et al (50, 51) studied platelet interaction with uncharged hydrophobic polymers using a controlled flow chamber. A correlation was found between increasing platelet adhesion and increasing critical surface tension of the polymer surface. At longer exposure times, Friedman et al. (16) found no correlation between critical surface and platelet adhesion.

The above discussion indicates that blood compatibility of biomaterials is not clearly correlated with any single surface property.

2.3 Platelet Adhesion

2.3.1 Uncontrolled Flow Conditions

Work has been done studying platelet adhesion (23, 24, 52-59) by medically orientated researchers. This work has been largely interested in pathological conditions of platelet adhesion and has therefore not attempted to take into account the importance of flow parameters and surface kinetics. The two most prominent experimental designs of this group are the rotating bulb (56, 59) and the glass bead column (52, 55).

In the original experiments (59) using the rotating bulb, a sample of anticoagulated blood was placed in a siliconized or vaseline bulb with an uncoated glass window and rotated at low speeds for long periods of time. This method has several drawbacks. The flow conditions are not well defined and in no way are representative of physiological blood flow. There is no guarantee that the adhesion is restricted to the uncoated

glass surface and the presence of a continual blood/air interface is bound to introduce unknown complications.

Hellem (52) has measured platelet adhesion in citrated whole blood using a glass bead column. In this experiment, 1 ml. of citrated blood is pumped to a plastic tubing and contacted with approximately 5 grams of glass beads for 30 seconds. Various problems make data using this technique difficult to interpret. The presence of an anticoagulent, an air interface and undetermined surface area available for the adhesion process are problems common to the rotating bulb method. This method also makes no allowance for the possibility of platelet entrapment. Finally it has been suggested (55) that the type of plastic used to make the column can play a significant role in determining the level of platelet adhesion.

Hirsh et al. (60) compared these two methods and found that while the absolute number of adhering platelets varied with the method employed overall trends were distinguishable. As the packed red cell volume increased from 12% to 67% the platelet adhesiveness (as measured by a percentage decrease in platelet concentration) was found to increase from 12% to 66%. Also increasing the level of the anticoagulent citrate decreased the levels of adhesion.

Besides the shortcomings already mentioned in connection with these designs the major reason for not using them to determine the thromboresistance of surfaces is their neglect of, or inability to estimate, the importance of flow parameters and surface kinetics.

One of the most important papers on platelet adhesion with uncontrolled flow conditions is by Cazenave et al. (58). In this work, one milliliter of platelet suspension was added to a collagen coated tube and rotated at 15 r.p.m. for 10 minutes at 22°C. Apyrase, known to degrade ADP, was added to the suspending medium to inhibit aggregation and thereby permitted the evaluation of adhesion in the absence of platelet aggregation. The number of adherent platelets was found to increase with platelet bulk concentration. These investigators found platelet adhesion increased with exposure time up to approximately 20 minutes after which it remained constant. The authors further detailed the effect of apyrase concentration, pH of suspending medium, temperature and divalent cations on platelet adhesion. More description about these variables will be given in the next chapter. This work is instrumental as it indicates the possibility of quantifying platelet adhesion without aggregation and presents the optimal conditions for many of the parameters involved.

2.3.2. Controlled Flow Conditions

a) Effects of Fluid Mechanics.

More recently the importance of flow, convective diffusion and chemical kinetics in platelet adhesion has been demonstrated (16-19, 25, 26, 50, 51, 61, 62). Platelet adhesion and subsequent thrombus formation occurs in arterio-venous shunts in laboratory animals (16-19, 61) and has been shown to form in regions of flow disturbances, separation and stagnation

(61, 63). In each case, an extracorporeal circuit was used with either canine or human blood and care was taken to eliminate any air/blood interfaces which may cause protein denaturation and elevated levels of platelet adhesion (50, 51).

Lyman et al. (50, 51) and Friedman et al. (16) conducted their experiments in extracorporeal flow chambers. Lyman's cell, constructed of Pyrex with a volume of 10 ml., was connected to a human vein by means of silastic tubing. The cell was designed so that polymer surfaces could either replace the glass surface or be administered to glass and then positioned in the cell. After the experiment, the cell was rinsed and fixed with absolute methanol. The surfaces were then stained and representative fields of 20,000 μ^2 were examined by oil immersion microscopy.

Friedman's (16) flow chamber, connected from a canine femoral artery, had a "U-shaped" cross section. This cross section was derived by placing a glass cover slip in contact with a 0.125" teflon tubing. This design possessed the same flexibility as Lyman's and adhesion was determined by averaging the platelet counts from five different 900 μ^2 areas from each microphotograph.

In contrast to the flow chambers of Friedman (16) and Lyman (50, 51), Dutton (62) and Petschek (61) using a technique of stagnation point flow allowed blood from a canine artery or vein to impinge directly upon a microscope cover slide. The analysis of platelet adhesion was determined using reflected light microscopy. A window placed over the microscope slide

permitted continuous observation of thrombus formation. Different surfaces were examined by coating the glass microscope slides.

Baumgartner (25, 26) has performed experiments in vivo using rabbit aortas denuded of endothelium by a balloon catheter thus exposing the subendothelial surface. He also performed platelet adhesion experiments in vitro using a perfusion chamber and subendothelium. The levels of platelet adhesion and presence of mural thrombi were evaluated quantitatively by employing morphometric measurements.

Turitto and Leonard (19) measured platelet adhesion to a spinning surface. In these experiments either a canine femoral artery and vein or the carotid artery and jugular vein were cannulated with teflon tubing (O.D. = .125"). By means of a three way stopcock, blood was able to flow continuously between artery and vein or be diverted to the flow chamber. A glass cover slip was attached to a disc face on the end of a supporting shaft in the flow chamber. This shaft was driven by an electric motor which had a variable speed range. An air/blood interface was avoided by having the disc placed in a slight recess in the flow chamber.

Baumgartner (25), Petschek et al. (61) and Friedman et al. (16) observed increases in platelet adhesion with increasing shear rates. This indicates the importance of convection and diffusion in platelet adhesion. As pointed out by Grabowski (17), if surface kinetics alone dominated we would expect platelet adhesion to be independent of shear rate. Turitto and Leonard (19) also witnessed an increase in platelet

adhesion with increasing shear rate. This effect was only observable for exposure times exceeding 120 sec. and suggested the possibility that platelet adhesion is governed by both diffusion and chemical kinetics.

If the diffusion process is instrumental in platelet adhesion, we would expect the levels of adhesion to be a function of bulk platelet concentration. Lyman et al. (51) did not find such a dependence but their experimental platelet concentration did not vary over a significant range. Friedman was also unable to determine an effect of platelet bulk concentration but apparently the scatter of measured values of bulk concentration could have hidden any fundamental relationship (17). However, Cazenave et al. (58) using a rotating bulb with platelet suspension, found a nonlinear increase in platelet adhesion with increasing bulk concentration.

All the above investigators (16-19, 50, 51, 58, 61, 62) observed that platelet adhesion increased with longer exposure times. The experiments of Turitto and Leonard (19) and Lyman et al. (50, 51) only lasted for a maximum time of four minutes while at least some of those of Dutton (62) and Petschek (61) lasted 15 minutes. Friedman et al. (16) and Baumgartner (25) reported platelet adhesion reaching an equilibrium value at approximately 20 minutes.

Lyman et al. (50, 51) reported that platelet adhesion had already commenced by 30 seconds. In agreement with this observation, Turitto and Leonard (19) have measured levels of adhesion after 10 seconds. Petschek (61), on the other hand, observed no platelet adhesion for the first minute of blood flow.

Despite the controversy over the exact onset of platelet adhesion, a uniform opinion exists that the adhesion process is random and forms a partially complete monolayer on artifical surfaces (16-19, 50, 51, 61, 62). On subendothelium surfaces, tho platelets form a continuous monolayer (25). The range of adhesion levels for artifical surfaces goes from 2 to 75 platelets/1000 μ^2.

Friedman et al. (16) further found that using heparin as an anticoagulent did not affect the level of platelet adhesion and the effect of increasing hematocrit produced a slight decrease in platelet adhesion. However, Baumgartner (25) found little platelet adhesion using platelet rich plasma (PRP) and Hirsch et al (60) as mentioned before, found increasing amounts of platelet adhesion with increasing hematocrit.

b) The Effect of Surface

The preceeding section has illustrated the importance of considering the effect of convective diffusion when attempting to quantify platelet adhesion. For trying to assess the role of chemical surface in platelet adhesion, the flow parameters must be controlled or erroneous conclusions concerning the thromboresistance of materials may be reached.

With the advent of vascular implants, investigators (17, 50, 51) became concerned with the influence of fluid mechanics on platelet adhesion and consequently most of the literature on platelet adhesion to polymer surfaces has been performed in well-defined fluid flow. Experiments that investigated the effect of surface on platelet adhesion without considera-

tion of fluid mechanics will not be reviewed here.

Lyman et al. (50, 51) observed that platelet adhesion decreased with decreasing critical surface tension as stated in the section on Biomaterials. These investigators also found that coating surfaces with albumin reduced platelet adhesion. This result has also been reported by other authors (58, 64). Lyman et al. further illustrated the importance of eliminating the Langmuir-Blodgett transfer of a denatured protein layer from the blood/air interface to the polymer surface. Failure to do so, resulted in inflated values of platelet adhesion and a lack of distinction between different surfaces.

Petschek has made a preliminary comparison between the effect of glass and polyurethane on platelet adhesion and thrombus formation. Canine blood, without an anticoagulent, was used and both surfaces experienced platelet adhesion followed by thrombus formation. Although no quantative comparison was made, it was noticed that more platelet aggregates and quicker formation of these aggregates were characteristic of glass.

Friedman et al. (17) have measured platelet adhesion on 16 different surfaces and found no appreciable differences. In all cases, the platelet adhesion increased with exposure time, up to approximately 20 minutes and then experienced a slight decrease. It should be noted that this experiment was run at a high shear rate of approximately 1000 sec^{-1} corresponding to arterial flow. These investigators also did not find any correlation between critical surface tension and platelet adhesion and concluded either that the platelet adhesion process

is diffusion controlled and therefore independent of the surface involved or that all the surfaces have become kinetically equivalent by adsorbing some substance prior to platelet adhesion. These experiments contrast with Lyman's finding that platelet adhesion does depend on the surface involved.

Turitto and Leonard (19) have attempted to reconcile these seemingly contradictory results. The classical theory for analysing the rotating disc equipment used by these authors predicts a linear increase in platelet adhesion with time. Since a non-linearity was observed, complex surface kinetics were assumed to be present. The experimental data was in good agreement with theoretical predictions when the platelet adhesion rate was assumed proprotional to the surface concentrations of both adherent protein and platelets adjacent to the surface. The authors then postulate that if protein adsorption is dependent on the chemical nature of the surface and subsequent platelet adhesion is not, Lyman's result of surface dependence at short times does not have to be viewed as antagonistic to Friedman's finding of surface inconsequentality at longer times.

CHAPTER 3

METHODS AND PROCEDURE

3.1 Equipment Design

The equipment used throughout the experimental work is shown in Figure 3.1. Two 5 cm. rods made of, or coated with the material to be tested are secured onto the two probes by means of a perspex threaded fastener. This fastener is 3/4" in length so that the presence of end effects will not significantly contribute to platelet adhesion on the rods. The internal diameter of the rods is only slightly larger than the diameter of the probe enabling a close fit to be obtained. The fittings are sealed by O-rings and only the outer surface area of the rod is available for platelet adhesion.

The platelet suspension is placed in glass tubes whose diameter is 22.6 mm. The two test tubes are attached to the supports by means of metal clamps These supports are adjustable by the screws shown on Figure 3.1. in order that the test tube may be centered with regard to the probe. A diameter of 22.6 mm. was chosen on the criteria of minimizing wall effects, variation in centering the probe and the amount of platelet suspension used.

The motor is a 115 volt, .35 amperes, D.C. electric motor capable of 400 revolutions per minute. This has been geared down to 200 revolutions per minute to provide smoother operation at low speeds. When the motor is switched on, the

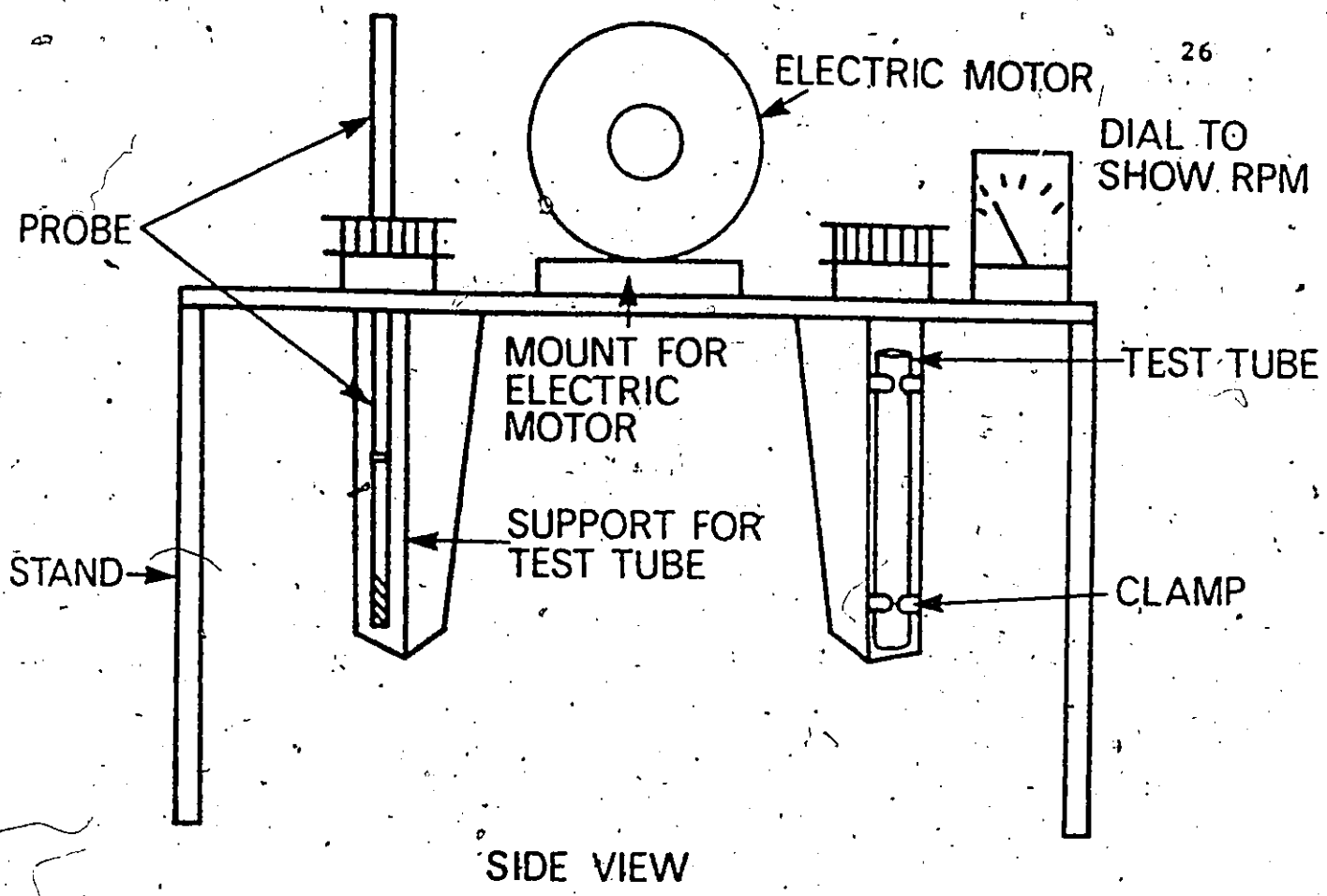

Figure 3.1 This is a schematic drawing of the experimental equipment. For simplicity, the right side probe and left hand test tube and clamps are not shown in the side view. Neither probes are in place in this top view. The scale if 5/16.

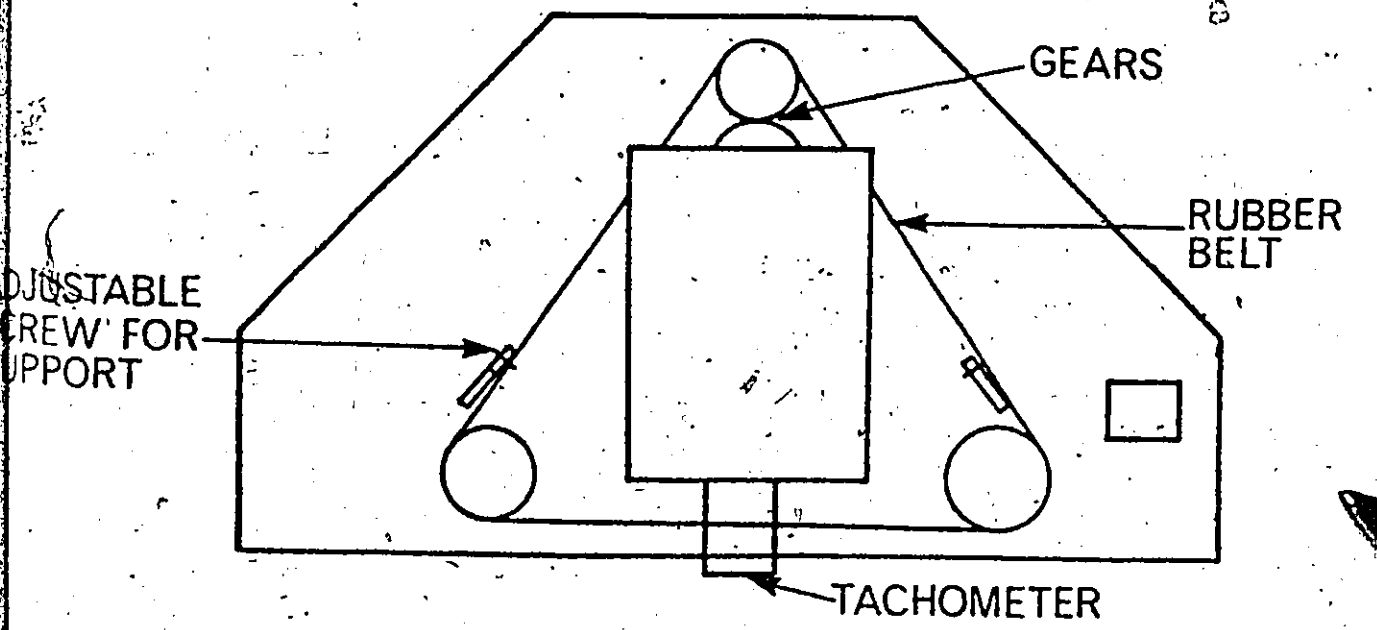

shaft which is connected to the driver causes the movement of a rubber belt. The motion of this belt rotates the two probes. A tachometer is connected to the shaft of the motor and the rotational speed is measured. Speed is controlled by a variable voltage D.C. power supply.

When the probe is aligned with the center line of the tube, and no eccentricity is present, the motion of the fluid may be referred to as Couette flow. This implies that no secondary flows exist and that the velocity components in the longitudinal and radial direction are zero. Preliminary visual investigation of the flow pattern using anisole as tracing particles have shown no secondary flows to be present.

In this system, the inner cylinder is rotating and the centrifugal force tends to introduce flow instability. As a result, the transition to turbulent flow occurs at a lower Reynolds number than for the case of a stationary inner cylinder and rotating outer cylinder. The stability of the system with an inner rotating cylinder was first investigated by Taylor (65). The conditions for unstable flow can be expressed with the aid of the Taylor number as shown in Schlichting (66).

$$T_a = \frac{U_i d}{\nu} \left(\frac{d}{R_1}\right)^{1/2} \geq 41.3 \text{ (viscous instability)} \qquad (3.1)$$

where d - the width of annulus

R_1 - radius of inner cylinder

U_i - peripheral velocity of inner cylinder

ν - kinematic viscosity

Even if the T_a number exceeds the stability limit this does not imply turbulent flow. Three different flow regimes defined by regions of the Taylor number are as follows (66).

$T_a < 41.3$: laminar Couette flow

$41.3 < T_a < 400$: laminar flow with Taylor vortices

$T_a > 400$: turbulent flow.

Taking the following average values for the parameters in Equation (3.1)

$U_i = 3.66$ cm./sec.

$\nu = .04$ poise/1.0 g/cc.

$d = .43$ cm.

$R_1 = .35$ cm.

We obtain $T_a = 39.4$.

From the above it may be concluded that the equipment operates in the laminar Couette flow regime. At higher rotational speeds or using less viscous suspensions the possibility of Taylor vortices does exist. However, in all cases, the flow will remain laminar.

3.2 Platelet Suspension

Pig platelets were used in all experiments. The pig blood was obtained from Canada Packers Ltd. (Toronto). The use of pig platelets should not prejudice the applicability of

results to human platelets as very little difference has been reported in experiments comparing adhesion between pig, rabbit and human platelets (58). The platelet suspension preparation follows that of Cazenave et al. (58).

Blood is collected from the carotid artery into plastic bottles containing the anticoagulant acid citrate dextrose (ACDS). The blood is centrifuged at 1600 r.p.m. for 15 minutes to separate the plasma from the red blood cells. The plasma is further centrifuged at 3200 r.p.m. for 15 minutes to permit the separation of the platelets from the supernatant. The platelets are then suspended in 10 ml Tyrodes Albumin solution* with 0.2 ml heparin and 0.1 ml apyrase.

Apyrase is added to the suspending medium to degrade any ADP present thereby preventing aggregation from this source. An apyrase concentration of 4 u2/ml was termed sufficient (58).

At this stage 350 u Ci of Cr^{51} (sodium chromate, activity 1 u Ci/u1) are added to the suspension. The test tube containing the suspension is then sealed and kept at 37°C. This temperature allows optimum chromate transfer to the platelets (67). Furthermore, chromium labelling at the level used here does not appear to affect platelet viability (68). Kattlove and Spaet (68) found that while chromium inhibited connective tissue induced aggregation, by inhibiting the release of platelet nucleotides, serotonin and platelet factor III, it had no effect on platelet-connective tissue adhesion. These investigators

---

* The composition of this solution may be found in Appendix A.

also found that ADP induced aggregation was only slightly affected while thrombin induced aggregation was unaffected by chromium. In conclusion, they report that the amount of chromium which must be bound to platelets to inhibit their functions is 10-100 times greater than that bound under normal labelling conditions and that the site of chromium binding to platelets is probably intracellular.

Tsukada et al. (69) report that Cr^{51} uptake by platelets is mediated by a bimodal transport mechanism with a diffusional and a saturable transport component. At the levels of chromium concentration used in the present work, chromium does not bind preferentially to any subpopulation of platelets (69, 70). Further information on the kinetics of isotopically labelled platelets may be found in the article by Aster (71). Labelling with Cr^{51} is therefore seen not to affect platelet viability or to bind preferentially.

The labelled suspension is now centrifuged at 2900 r.p.m. for 10 minutes. The platelets are separated from the supernatant and resuspended in the same amount of Tyrode Albumin and apyrase used earlier. The supernatant which contains the free Cr^{51} is discarded.

After waiting 15 minutes so that the platelets regain their normal shape, the suspension is centrifuged again and the platelets separated from the supernatant. The platelets are then resuspended in the same concentrations of Tyrodes Albumin and apyrase. The platelet concentration is then counted using a hemocytometer and ammonium oxalate for a counting solution.

After this the platelet suspension may be diluted with Tyrodes Albumin to the desired platelet concentration.

Approximately 200 ml of packed red blood cells are removed from the centrifuged pig blood. The red blood cells are carefully separated from the plasma and centrifuged at 3600 r.p.m. for 12 minutes to remove any remaining plasma and white blood cells. After the supernatant has been removed, the red blood cells are suspended in 4 ml of Tyrodes Albumin solution and 1 ml ACDS. This washing procedure of centrifuging and resuspending is repeated three times. The hematocrit is then determined and a specified volume of the red blood suspension added to the platelet suspension to produce a final suspension with a predetermined platelet count and hematocrit.

Due to the complex and largely undetermined interactions between platelets and plasma proteins (see Chapter 2) the suspending medium used throughout this work contained no plasma proteins except albumin. The presence of albumin maintained the desired osmotic pressure.

Several advantages exist with this suspending medium. It permits a wide range of platelet concentrations and hematocrits to be observed and the protein composition may also be controlled. Secondly, with the removal of fibrinogen from the suspending medium, there is little chance of stimulating the pig platelets to aggregate because fibrinogen is necessary for the aggregation of pig platelets (72, 73). Finally, our experiments using this suspension may be run for long periods of time without having to add an anticoagulent. This is important as the effect

of anticoagulents on platelet adhesion has not been clearly established. For example, EDTA (ethylenediaminetetraacetate); an anticoagulent, has been shown to inhibit platelet adhesion (23, 24, 55, 58). The suspected cause of this inhibition is the chelating of the divalent cation Ca^{++}. On the other hand, there is some evidence that heparin does not affect platelet adhesion (17, 23, 55). Free Ca^{++} is present in our platelet suspending medium.

The viability of platelets and red cells were checked by morphological examination both before and after an experiment and no irregularities were observed. After all the experiments using a given aliquot have been perfotmed, 2 ml of the aliquot are centrifuged to remove the red cells and platelets. Investigation of this supernatant can provide more information about the condition of the cellular constituents.

The intactness of the red cell membrane was examined by testing the supernatant for hemoglobin by UV spectrophotometry. Since only trace amounts (< 1 mg %) of hemoglobin were detected, it may be concluded that no substantial amount of hemolysis has occurred.

In the platelet preparation free Cr^{51} is removed, though 1-5% remains, and the radioactivity of the supernatant indicates the amount of lysis that the platelets have undergone. The average supernatant values for 3 randomly chosen days are shown in Table 3.2.1.

This data demonstrates that the platelets did not release their grannule contents nor were their membranes

No. of Supernatants Examined on 1 Day	$\bar{x} \pm$ S.D. (% of Total Solution Counts)
8	$2.8 \pm .6$
3	$4.2 \pm .2$
4	$4.9 \pm .7$

Table 3.2.1 Supernatant Radioactivity.

significantly damaged. The supernatant radioactivity never exceeded 7% of the total solution radioactivity.

Before each experiment, platelet function was examined by an aggregation test. The aggregation of pig platelets upon the addition of 100 µl. of 5×10^{-5}m ADP and 50 µl. of 2% human fibrinogen suggested no loss of platelet function. The chart output from one aggregation test may be found in Appendix D.

3.3 Selection and Preparation of Biomaterials

3.3.1 Selection

The materials that were selected for examination were chosen either as control surfaces or as possible thrombo-resistant surfaces.

To check the operating characteristics of the experimental apparatus, platelet adhesion to glass and collagen coated glass were compared. It is known that platelets have a strong affinity for collagen (74) and it is therefore expected that platelet adhesion to collagen would exceed adhesion to

glass (58). A quantitative and reproducible difference would indicate, to a first approximation, a suitable and reliable design. These two surfaces may also be used as control surfaces with which to compare other biomaterials since platelet activity varies daily. An abundance of adhesion data exists for collagen and glass in undefined flow regimes and it was hoped that by controlling flow parameters any fundamental differences would be elucidated.

Polymers have been preferentially selected over other materials for vascular implants because of their accessibility, relative inertness, and wide range of mechanical properties.

It must be decided which criteria (see preceeding chapter) will be chosen to provide surfaces for quantitative examination of platelet adhesion. Following the work of Lyman et al. (49-51), indicating low levels of platelet adhesion to uncharged hydrophobic polymers, polystyrene and polyurethane were selected. Sulphonated polystyrene was chosen because of its known thromboresistant properties (48).

3.3.2 Preparation of Biomaterials

a) Glass

Glass rods (O.D. = 7 mm.), cut into 5 cm. lengths were washed in HCl (IN) and alcoholic potassium hydroxide (IN) and dried at 100°C for not less than 2 hours in a dust free oven.

b) Collagen Coated Glass

The collagen coating was applied to clean, dry glass rods (see above). The acid soluble collagen solution was prepared

by the technique of Cazenave et al. (58) and is known to retain its activity for 3-4 months. The glass rods were immersed in the collagen solution for 5 minutes at 22°C, subsequently removed and rinsed by dipping four times in plain Tyrodes solution. The rinse treatment also raises the pH to 7.4 and allows reconstitution of the collagen fibers. After a 15 minute drying time, the collagen coated rods were ready for use. This application procedure closely follows that of Cazenave et al. (58) and results in collagen being polymerized in a fibrous manner on glass. Microscopic observations revealed an even coating of collagen (see pages 55, 56).

c) Albumin Coated Glass

Glass rods were predipped for 2 minutes in Tris buffer* and then immersed in a 50 mg.% solution of albumin in Tris buffer for at least 2 hours. The albumin coated rods were then rinsed for 15 minutes in Tris buffer. The Tris buffer was changed and the rinse procedure repeated.

d) Polymer Coated Delrin

Sample rods constructed entirely of polyurethane were too flexible to be secured to the probes and polymer coatings would not adhere firmly to glass. Therefore, delrin was used as a carrier substance for the various polymers.

The polyurethanes used were synthesized in this laboratory (75). The sulphonated polystyrene and polystyrene were obtained elsewhere (76, 77).

---

* The composition of Tris buffer may be found in Appendix A.

The sulphonated polystyrene and polystyrene coatings are applied by twice dipping the delrin rods into solutions of the polymers in dimethylsulphoxide and allowing them to dry at room temperature for one hour. The polyurethane coating is administered by dipping four times in the prepared solution and allowing to dry overnight at 60°C.

The delrin carrier rods were reused after removing the polymer coating and were checked continually for residual radioactivity. The application of a uniform coat is important to avoid cellular destruction, increased surface area and platelet entrapment.

3.4 Operational Procedure

Before the probes are placed in the platelet suspension, they are predipped for 2 minutes in Tyrodes solution. This is to prevent Langmuir-Blodgett transfer of a partial monolayer of denatured protein and platelets as the probe is placed in the suspension. The importance of this transfer has been recognized (51) and predipping represents a means of reducing the effect of the air/suspension interface.

After the probes have been rotated in the platelet suspension for the desired period of time and excess fluid removed by shaking, they are rinsed in Tyrodes solution for 30 sec. at 100 r.p.m.

The surface to be tested is then put in a plastic vial and placed in a Beckman Biogamma Counting System. This is a gamma radiation counter which has a variable discriminator

modulus enabling the selective counting of the desired isotope. The counting time can also be varied. Since radioactive decay with a short half life follows a Poisson distribution (78), increased counting times will reduce the fractional error. Sufficient counts were obtained by allowing two minutes for counting.

CHAPTER 4

THEORETICAL MODEL

In this chapter, a theoretical model will be discussed to describe platelet adhesion in a Couette flow environment. The model will have to account for the possibilities of surfaces having different reactivities toward the adhesion process and of a diffusion coefficient much larger than the one predicted by Brownian motion.

In the next chapter, the model will be compared with the experimental data to try and elucidate the mechanism of platelet adhesion. Nonlinear least squares will be used to estimate an effective platelet diffusion coefficient and to determine if this diffusivity is a function of shear rates and hematocrit.

We will begin the analysis by stating the assumptions and simplifications used.

1. The platelet/red blood cell suspension will be assumed to be incompressible and homogeneous.

This assumption implies that a continuum approach may be taken and that the cellular nature of blood may be ignored. If, as will be shown later, the concentation boundary layer is much thicker than a red cell diameter the assumption is valid.

2. The flow is laminar.
3. There is no eccentricity of the probe.
4. There are no Taylor vortices.

Assumptions 2-4 ensure that no secondary flows are present and are justified by the calculated Taylor number and visual observations (refer to Chapter 3).

5. Platelet bulk concentration is uniform.

6. Platelets are neither created or destroyed.

7. Platelet adhesion is not a function of age, size or radioactive label.

The justification of the assumption that platelet adhesion is uniform throughout the population is given in Chapter 3.

8. The system may be approximated by rectangular co-ordinates.

This assumption may be justified if the concentration boundary layer is small compared to the radius of the rod.

9. There are no convective flows present, since this is a Couette flow apparatus.

10. The flow is steady.

11. The platelet/red cell suspension will be assumed to behave in a Newtonian fashion.

This assumption is justified as it has been reported that red cell suspensions in normal saline are nearly Newtonian without any measurable yield value (3). A possible explanation of this phenomenon is the absence of fibrinogen which reduces red cell aggregation and thereby eliminates a major contribution to the non-Newtonian behaviour of blood (3).

12. At the surface, the platelet arrival rate will be equated to platelet adhesion which is assumed to be first order with respect to platelet concentration and independent of the

surface area available. Obviously this boundary condition is only exact initially and becomes increasingly invalid as the level of adhesion increases. At high levels of adhesion, the process is selective and is not described by the above boundary condition which predicts random behaviour. The boundary condition is probably adequate for low levels of adhesion.

The general mass balance for platelet conservation is given as (79)

$$\frac{Dc}{Dt} = \nabla \cdot (D_p \nabla c) \qquad (4.1)$$

where

$\frac{D}{Dt}$ - material derivative

D_p - platelet diffusivity

c - platelet concentration.

Equation (4.1) reduces to

$$\frac{\partial c}{\partial t} = D_p \frac{\partial^2 c}{\partial x^2} \qquad (4.2)$$

for the one dimensional case of Couette flow in Cartesian co-ordinates.

The boundary conditions are as follows.

1. The bulk platelet concentration will be taken to be

$c = C_o$ at $t = 0$ for all x

where C_o = initial concentration (platelets/cm^3)

2. The boundary condition described in assumption #12 is given mathematically as

$$-D_p \frac{\partial c}{\partial x} = kc \qquad \text{at } x = 0$$

where k = apparent wall adhesion constant (cm./sec.)

3. $c = C_o$ at $x = \infty$ for $t > 0$.

The solution to Equation (4.2) with boundary conditions 1-3 is given by Carslaw and Jaeger (80)

$$\frac{c}{C_o} = \text{erf} \frac{x}{2\sqrt{D_p t}} + e^{\frac{k}{D_p} x + \frac{k^2 t}{D_p}} \{\text{erfc} (\frac{x}{2\sqrt{D_p t}} + \frac{k}{D_p} \sqrt{D_p t})\} \tag{4.3}$$

where erf is written for the error function and is expressed mathematically as

$$\text{erf}(z) = \frac{2}{\pi^{\frac{1}{2}}} \int_0^z e^{-n^2} dn$$

with the following properties

$$\text{erfc}(z) = 1 - \text{erf}(z)$$

$$\text{erf}(-z) = -\text{erf}(z), \text{erf}(0) = 0, \text{erf}(\infty) = 1$$

The platelet concentration adjacent to the surface is given by evaluating Equation (4.3) at $x = 0$

$$c|_{x=0} = C_o e^{\frac{k^2 t}{D_p}} \text{erfc} (\frac{k}{D_p} \sqrt{D_p t}) \tag{4.4}$$

To find the flux to the wall we could proceed by differentiating (4.4). A simpler approach is to use boundary condition (2).

$$\text{Flux to wall} = kc\big|_{x=0} \qquad (4.5)$$

The flux to the wall is equal to the rate of change of surface concentration.

$$J = \frac{ds}{dt} = k\,C_o\,e^{+\frac{k^2 t}{D_p}}\,(1 - \operatorname{erf}(\frac{k}{D_p}\sqrt{D_p t})) \qquad (4.6)$$

where J = flux to the wall (pl/cm^2.sec.)

s = platelet surface density (platelets/cm^2.)

Integrating Equation (4.6) with time

$$S = \int_o^t k\,C_o\,e^{\frac{k^2 t}{D_p}}\,(1 - \operatorname{erf}(\frac{k}{D_p}\sqrt{D_p t}))dt \qquad (4.7)$$

At large values of $\frac{k}{D_p}\sqrt{D_p t}$, corresponding to the diffusion controlled case, the following asymptotic formula may be used (81).

$$\exp(z^2)\operatorname{erfc}(z) = \frac{1}{\pi^{\frac{1}{2}}}(\frac{1}{z} - \frac{1}{2z^3} + \frac{1\cdot 3}{2^2\cdot z^5} \cdots) \qquad (4.8)$$

Substituting only the first term of the right hand side of Equation (4.8) into Equation (4.7) to obtain

$$S = \int_o^t k\,\frac{C_o D_p}{\pi^{\frac{1}{2}} k\sqrt{D_p t}}\,dt \qquad (4.9)$$

or

$$S = 2\,C_o\,(\frac{D_p t}{\pi})^{\frac{1}{2}} \qquad (4.10)$$

The equation expresses the cumulative platelet surface density for the diffusion limited case and is plotted in Figure 4.1.1 for various diffusivities.

For the other limiting case when surface and bulk concentrations are not significantly different Equation (4.6) becomes

$$J = k C_o \tag{4.11}$$

The platelet diffusivity may be estimated by fitting the experimental data to Equation (4.10) using nonlinear least squares. Before this is done the validity of using rectangular co-ordinates must be tested. For the diffusion limited case Equation (4.3) reduces to

$$c = C_o \operatorname{erf} \frac{x}{2\sqrt{D_p t}} \tag{4.12}$$

This equation is used to plot the concentration profiles for three diffusivities as shown in Figures 4.1.2-4.1.4.

From these plots the boundary layer (thickness at which .95 of the bulk concentration is reached) is largest at a diffusivity of 1.0×10^{-7} cm^2./sec. and a time of 10 minutes. This maximum value is approximately 250 microns and is small compared to the 3500 micron radius of the rod. Therefore, the error involved in approximating the system by rectangular co-ordinates will be small.

The concentration profiles also show the minimum boundary layer thickness to be approximately 25 microns. This

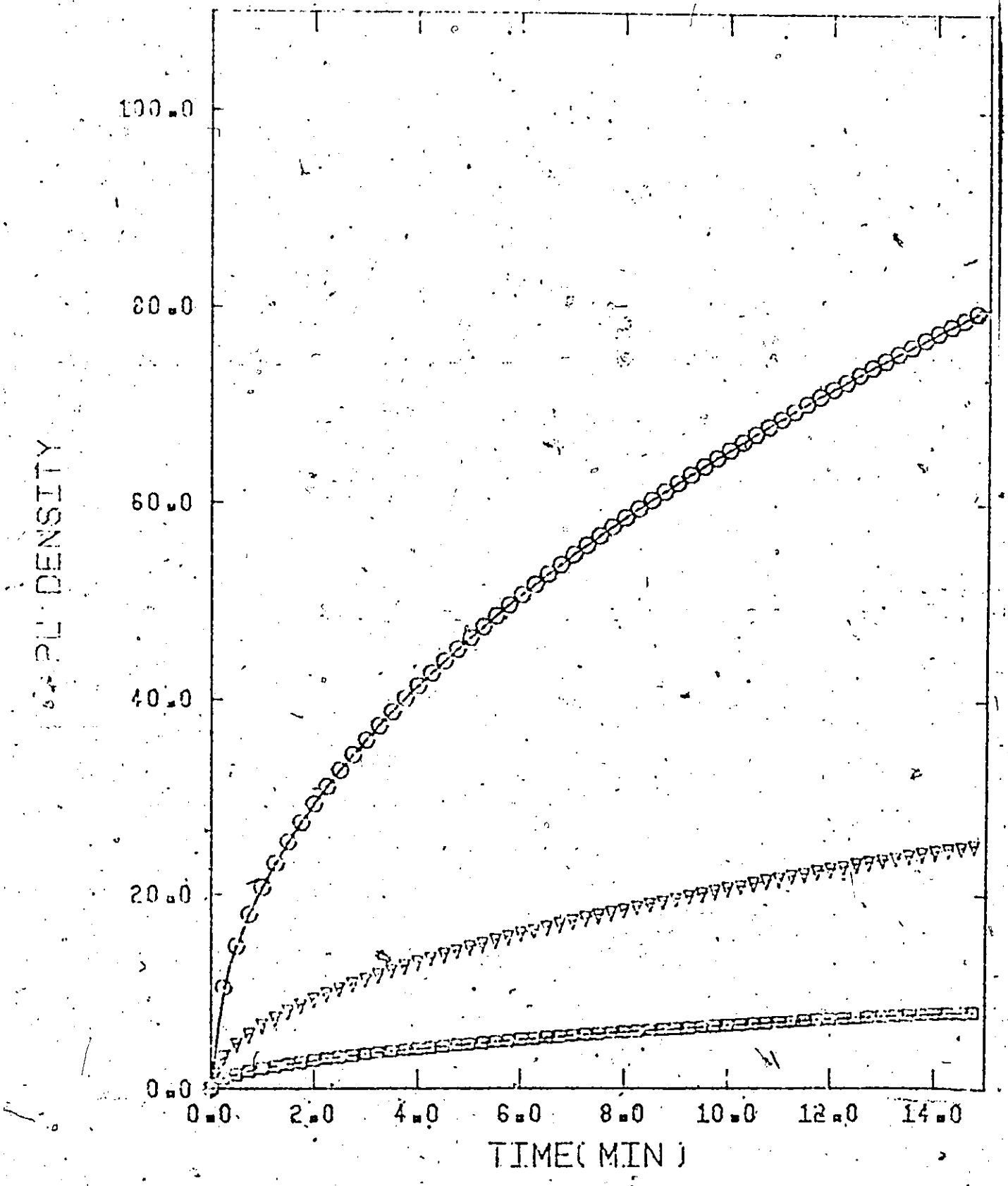

Figure 4.1.1. Theoretical Predictions of Platelet Adhesion for the Diffusion Limited Case with Diffusivities of 1.0×10^{-9} cm^2./sec. (□), 1.0×10^{-8} $\frac{cm^2}{sec}$ (▽) and 1.0×10^{-7} $\frac{cm^2}{sec.}$ (○).

Platelet density = platelets /1000 μ^2.

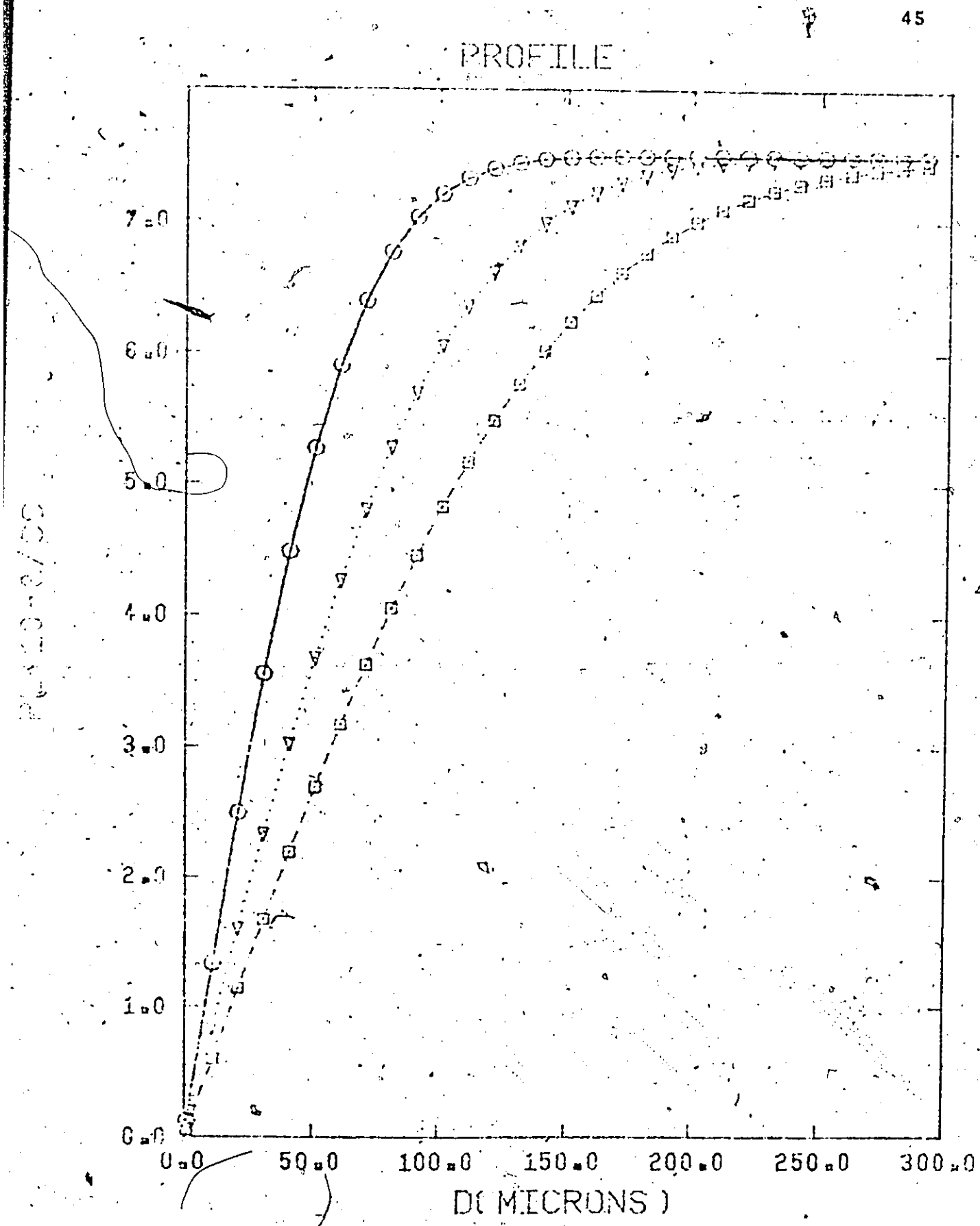

Figure 4.1.2. Platelet Concentration Profiles with an Assumed Platelet Diffusivity of 1.0×10^{-7} $cm^2/sec.$, at Times of 2 (0), 5 (▽) and 10 (□) Minutes.

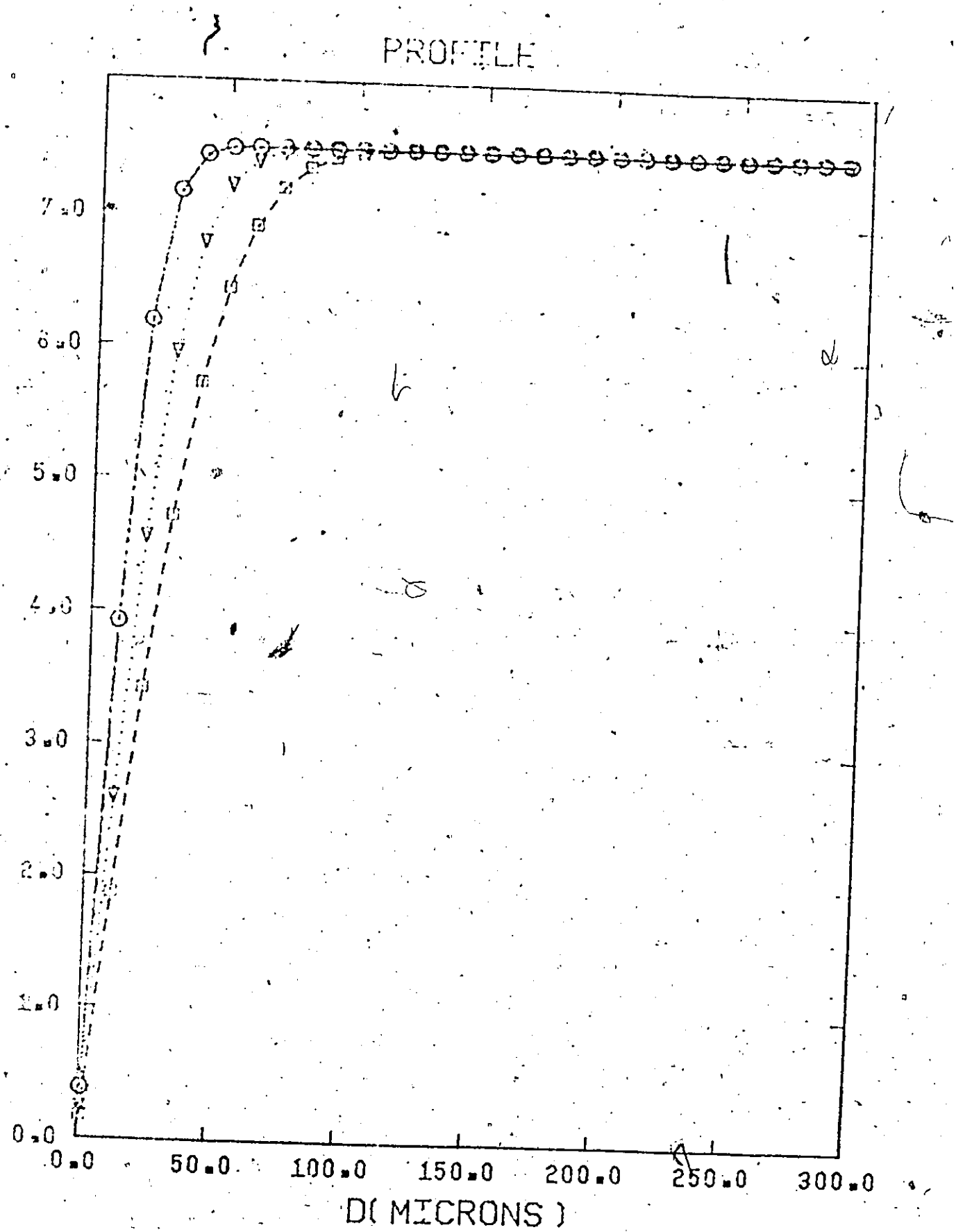

Figure 4.1.3. Platelet Concentration Profiles with an Assumed Platelet Diffusivity of 1.0×10^{-8} cm^2./sec. at Times of 2 (O), 5 (V) and 10 (□) Minutes.

Figure 4.1.4. Platelet Concentration Profiles with an Assumed Platelet Diffusivity of 1.0×10^{-9} cm^2./sec. at Time of 2 (O), 5 (▽) and 10 (□) Minutes.

is three times the radius of a red cell and serves as justification for using the continuum approach.

The solution for Equation (4.2) in cylindrical co-ordinates with boundary conditions 1-3 is given in terms of Bessel functions (80).

The adhesion data for all surfaces, except collagen, appears to reach a limiting platelet surface density. Boundary condition (2) does not take account of this phenomena. A more appropriate boundary condition is given by

$$-D_p \frac{\partial c}{\partial x} = kcf \quad \text{at } x = 0 \quad t > 0 \tag{4.13}$$

where f = fractional surface area not yet covered by platelets.

Furthermore

$$f = 1 - \frac{1}{S_p} \int_0^t -D \frac{\partial c}{\partial x}\Big|_{x=0} dt \qquad t \geq 0 \tag{4.14}$$

where S_p = equilibrium platelet surface density.

Grabowski (17) has questioned the validity of boundary Equation (4.13) and concluded that it is probably valid only for low degrees of surface coverage.

For the reaction limited case

$$J = kcf$$

or

$$\frac{dS}{dt} = kc \left(1 - \frac{S}{S_p}\right)$$

which may be integrated to give

$$S = S_p (1 - e^{-kct/S_p}) \qquad (4.15)$$

The Brownian diffusivity for large spherical particles may be calculated from the following equation (79).

$$D_B = \frac{k_B T}{6\pi b \mu}$$

where k_B = Boltzman's constant (1.38×10^{-16} $\frac{gm\ cm^2.}{sec^2.}$)

T = temperature ($295^{\circ}K$)

μ = viscosity (1.5×10^{-2} gm/cm-sec.)

b = particle radius (1.0×10^{-4} cm.)

$$D_B = 1.4 \times 10^{-9}\ cm^2./sec.$$

Red blood cells are known to undergo translation, rotation and deformation when subjected to a shear force (1-3, 14). It has been postulated that the diffusivity of platelets will be augmented by this additional motion (5, 6). Several authors (4-6) have proposed a linear dependence between platelet diffusivity and shear rate. Grabowski et al. (18) have assumed a power law relationship to shear rate which is expressed mathematically as

$$D_p \propto \left(\sqrt{\left(\frac{du}{dr}\right)^2}\right)^m \qquad (4.16)$$

where the exponent m is expected to take on some value between zero and one (18).

Grabowski et al. (18) have found platelet diffusivity to be shear rate dependent while Turitto and Leonard (19) suggest that any dependence on flow conditions is very weak.

The initial model assumed, in this work, to account for the possibilities of a shear rate dependence and cell-cell interactions is expressed mathematically as

$$D_p = H^{\beta} \dot{\gamma}^{\eta} \tag{4.17}$$

where $\dot{\gamma}$ = shear rate (sec^{-1})

H = hematocrit

β = constant

η = constant

Equation (4.17) will be fit by least squares to determine what, if any, effect shear rate and hematocrit have on platelet adhesion.

The calculations for converting the revolutions per minute to shear rate are shown in Appendix B.

CHAPTER 5

EXPERIMENTAL RESULTS

5.1 Selection of Operating Conditions

In order (1) to ensure the presence of Couette flow, (2) to determine a suitable operating temperature, (3) to examine platelet viability with respect to the duration of shear and (4) to check the validity of the radioactive counting method the following sets of experiments were performed.

5.1.1 Establishment of Couette Flow Conditions

Table 5.1.1 contains data on platelet surface density as a function of shear rate and test tube diameter.

Shear Rate (Sec^{-1})	Av $\pm$ S.D. Dia. = 14 mm.	Av $\pm$ S.D. Dia. = 15.8 mm.	Av $\pm$ S.D. Dia. = 22.6 mm.
0	2.05 $\pm$ .45	1.67 $\pm$ .34	3.45 $\pm$ .28
9.5	6.49 $\pm$ 1.16	4.52 $\pm$ .17	4.19 $\pm$ .22
19	12.5 $\pm$ .70	7.09 $\pm$ .87	4.14 $\pm$ .33

Table 5.1.1. Platelet Surface Density* as a Function of Shear Rate and Test Tube Diameter

Each result in Table 5.1.1 is the average value of four observations with the accompanying standard deviation.

* Expressed as platelets per 1000 μ^2.

Each observation was obtained from a collagen coated rod that was exposed for 15 minutes to red cell free platelet suspension. The platelet bulk concentration for the experiments in Table 5.1.1 was 750,000 pl/mm^3. This concentration was used in all subsequent experimental work unless otherwise noted. Each column represents results from a different batch of platelet suspension and due to the daily variation in the physical and chemical properties of pig platelets must stand on its own merit. It is not valid to compare the absolute values of platelet adhesion from day to day. Qualitative comparisons may be made between experiments of different days by using a control.

Using diameters of 14 mm. and 15.8 mm., platelet adhesion increased with increasing shear rate. This is not the expected behaviour of a Couette flow apparatus and may be accounted for by a platelet diffusivity dependence on shear rate or by an increase in secondary flows, due to poor alignment of the probe, and wall effects.

Platelet diffusivity is not likely to be shear rate dependent as this experiment was performed in the absence of red cells. Platelet adhesion appears to be independent of shear rate for the 22.6 mm. diameter. This justifies the assumption made in Chapter 4 that the effect of eccentricity can be neglected. The smaller variances associated with the 22.6 mm. diameter tube suggest that alignment and wall effects are no longer as critical as with the smaller diameter tubes.

5.1.2 Effect of Temperature

Although platelets in vivo function at 37°C it is experimentally convenient to operate at room temperature. However it was considered necessary to establish that significant differences in adhesion did not exist between 37°C and room temperature (approximately 22°C). The data in Table 5.1.2 show that the means are not statistically different for the two temperatures investigated.

Surface	Hemat.	Exposure	Shear Rate	T°C	Av. ± S.D.
Collagen	0%.	10 min.	19 sec^{-1}	22	7.9 ± 1.9
Collagen	0%	10 min.	19 sec^{-1}	37	7.2 ± .9

Table 5.1.2. Effect of Temperature on Platelet Adhesion*

5.1.3 Platelet Viability with Respect to Duration of Shear

Due to the fact that only a small volume (ca. 150 ml) of platelet suspension is available on a given day, it is necessary to use an aliquot of suspension more than once. Therefore experiments dealing with the effect of duration of shear on platelet adhesion were performed. Since the longest total duration of shear caused by re-use of aliquots was 35 minutes, the study was confined to this interval.

* Represent average of four observations (platelets/1000 μ^2)

Total Time (Min.)	Av. ± S.D. (PL/1000 μ^2)
0	40.1 ± 3.18
10	41.4 ± .92
20	38.1 ± 2.17
30	38.6 ± .89

Table 5.1.3. Effect of Duration of Shear on Platelet Adhesion to Collagen.

Table 5.1.3 contains the data for an experiment in which collagen-coated glass was exposed to a platelet/red blood cell (RBC) suspension of 20% hematocrit for 5 minutes at a shear rate of 19 sec^{-1}. This experiment was repeated four times with the same suspension at 10 minute intervals to determine if there is a change in platelet reactivity with duration of shear. Hypothesis testing of the means in Table 5.1.3 revealed no statistical differences at a 95% confidence level indicating that platelets suffer no, or very little, damage with a shear rate of 19 sec^{-1} and an exposure time of 40 minutes.

5.1.4 Comparison of Radioisotope Evaluation Technique and Microscopic Direct Counting

It is necessary to confirm that the radioactivity on the examined surface is due to the adherence of Cr^{51} labelled platelets and not to the adherence of free Cr^{51}. The electron micrographs on pages 55 and 56 not only demonstrate platelet adhesion but also provide an independent check of our surface

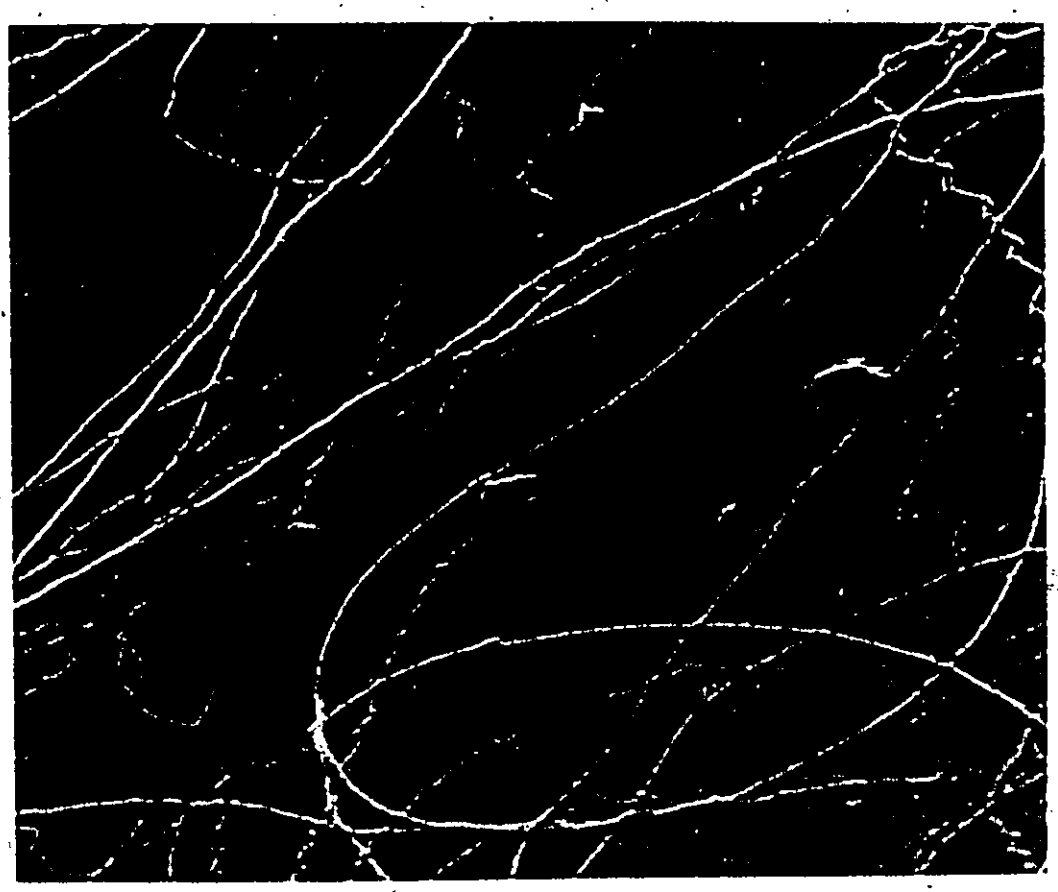

Figure 5.1.1. This is an electron micrograph of a collagen coated glass rod which was exposed to platelet/red cell suspension (hematocrit = 10%) for 2 min. The platelet bulk concentration is 750,000/mm^3. 40,000 magnification.

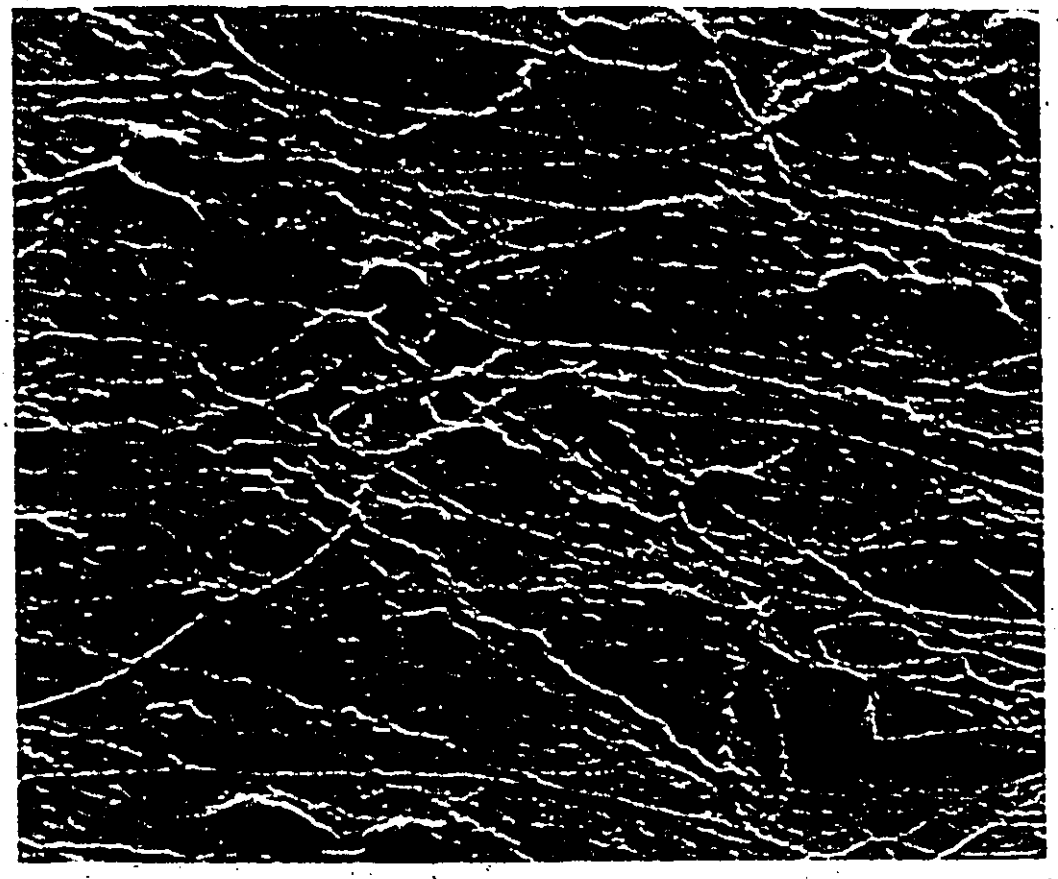

Figure 5.1.2. This is an electron micrograph of a collagen coated glass rod which was exposed to platelet/red cell suspension (hematocrit = 10%) for 30 minutes. The platelet bulk concentration is 750,000/mm^3. 40,000 magnification.

evaluation method. Knowing the magnification of the electron micrographs, the number of adherent platelets per 1000 μ^2 may be estimated.

Figure	Radioisotope*	Electron Micrograph*
5.1.1	15	20
5.1.2	89	100

*. Expressed as platelets/1000 μ^2

Table 5.1.4. Comparison of Counting Procedure.

Table 5.1.4 and Figures 5.1.1 and 5.1.2 indicate that the radioactivity on the surface is due to the adhesion of Cr^{51} labelled platelets. To further investigate the possibility of free Cr^{51} adhesion, a 100 ml. aliquot of platelet/red cell suspension was centrifuged after an experiment and the supernatant retained. The same experiment was performed again with the supernatant used in place of the cellular suspension. Surface radioactivity was reduced to about 5% of its normal value when supernatant was used instead of suspension. It is therefore inferred that no more than 5% of the radioactivity on a typical surface is a consequence of the adhesion of free Cr^{51}.

5.2 Effect of Shear Rate and Hematocrit

Platelet adhesion to glass and collagen coated glass has been found in this work to be augmented by the addition of

red cells. This increase may be seen in Figures 5.2.1-5.2.3 and may be accounted for by one of the two following mechanisms. Either red blood cells have released their adhesion promoting chemical components (eg., ADP) and thereby increased adhesion or they have augmented the platelet diffusivity through their radial fluctuations and rotational motions. The first hypothesis was initially presented by Gaarder et al. (34), who suggested that the adhesion of platelets from whole blood to glass depends on the release of ADP from red blood cells. The second hypothesis associates the increased levels of platelet adhesion with the physical properties of the red blood cell. This concept has been discussed in detail in Chapter 2.

To investigate the possibility of increased adhesion due to a chemical release from red cells, a glass surface was rotated for 5 minutes at 19 sec^{-1}, in a red blood cell suspension (without platelets) and then immersed and rotated under the same conditions in a red-cell-free platelet suspension. This procedure did not increase platelet adhesion indicating that if a chemical stimulus is present it is not mediated by the surface. The following additional facts also minimize the possibility of the presence of chemical stimulants. Apyrase is added to the platelet suspension and is responsible for degrading any free ADP. Also, the morphology of the red cells was found to be normal. It appears unlikely that a chemical release is responsible for the increased levels of platelet adhesion.

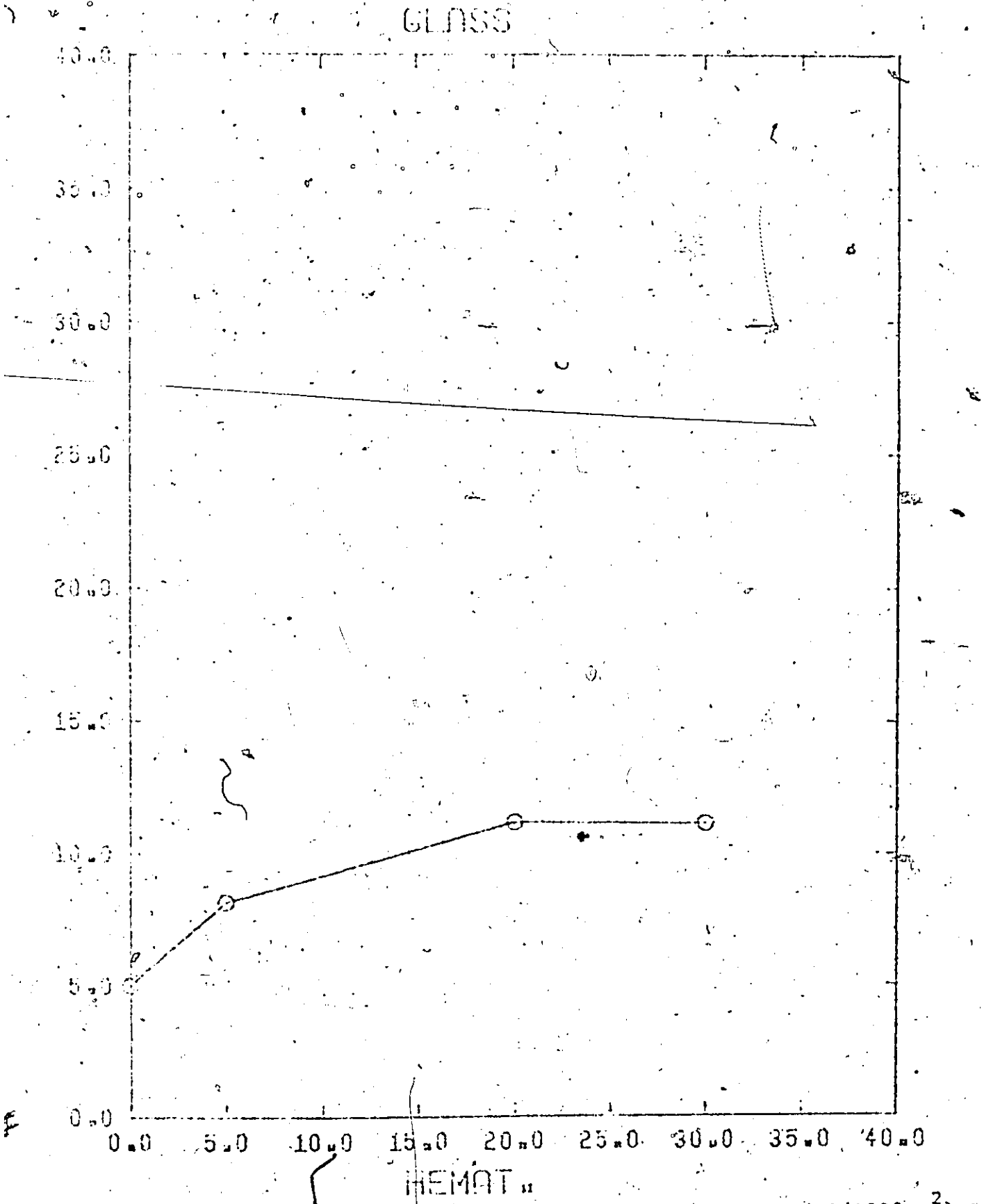

Figure 5.2.1. Plot of platelet surface density on glass (pl/1000 μ^2) against hematocrit. Each point is the average of two observations. The glass rods were exposed to the suspension for 10 minutes at a shear rate of 19 sec^{-1}.

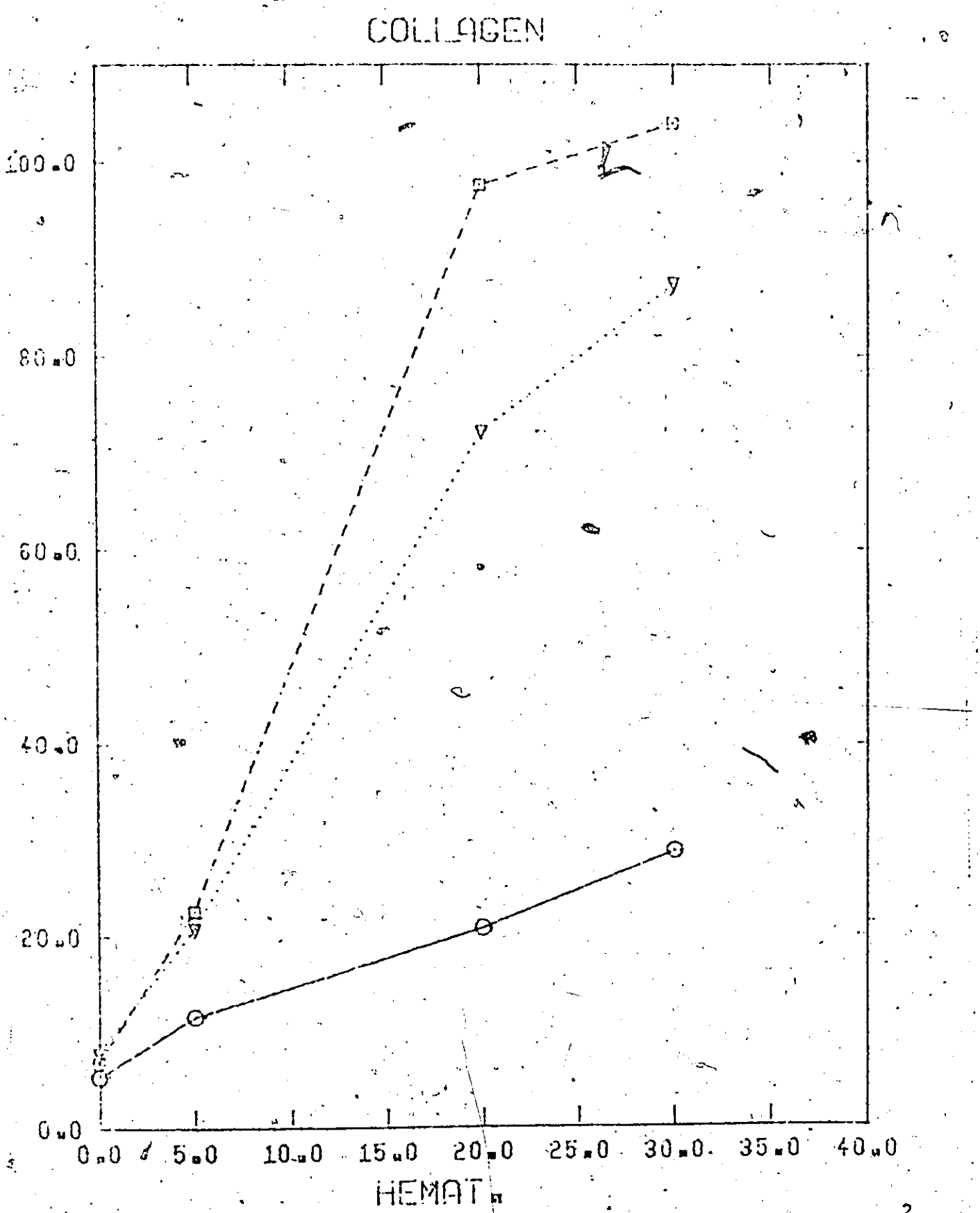

Figure 5.2.2. Plot of platelet surface density on collagen (pl/1000 μ^2) against hematocrit. Each point is the average of two observations and each sample was exposed to the suspension for 10 minutes. The three different shear rates examined were 9.55, 23.8 and 38.2 sec^{-1} and are designated as O, V, and □ respectively.

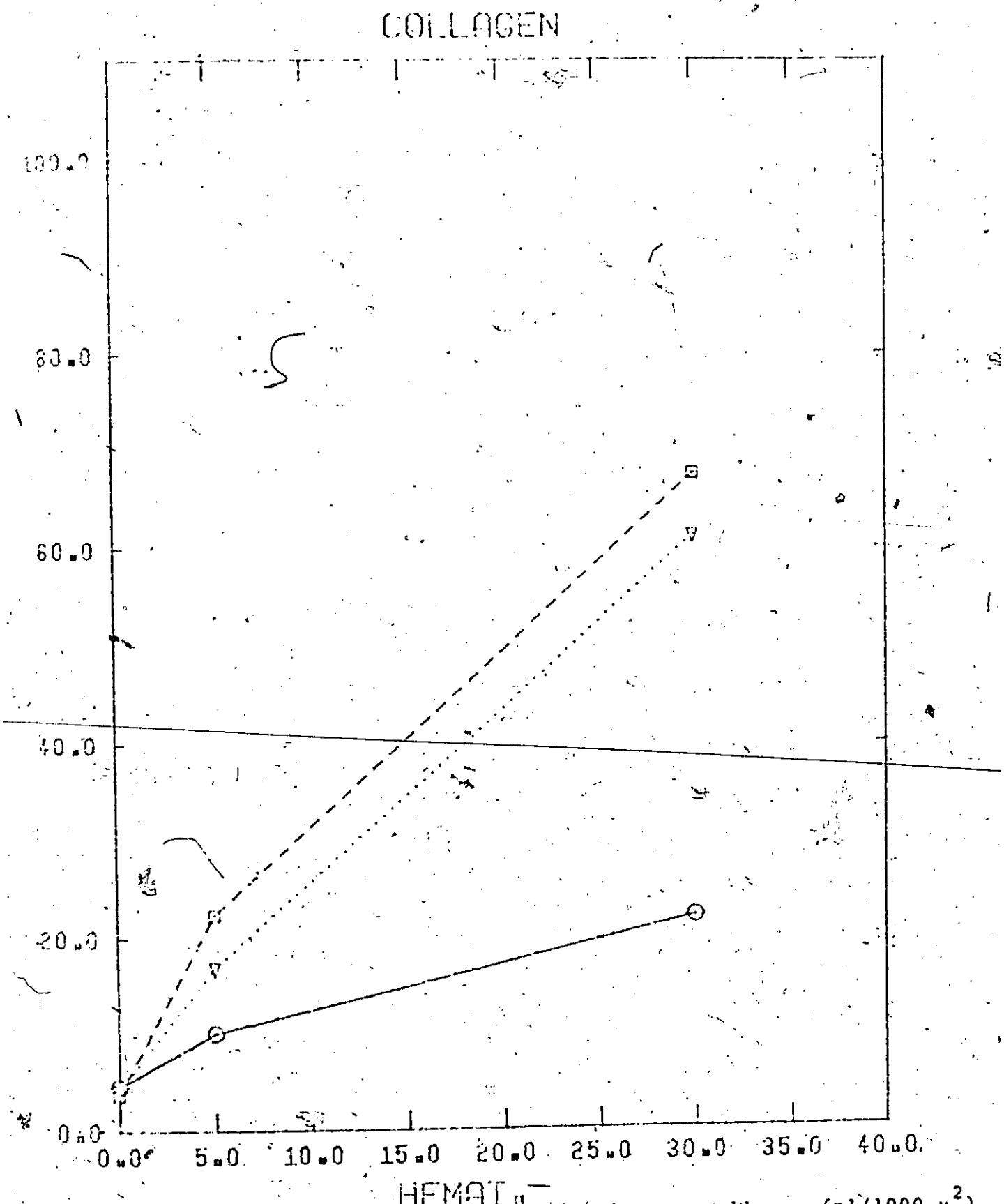

Figure 5.2.3. Plot of platelet surface density on collagen (pl/1000 μ^2) against hematocrit. Each point is the average of two observations and each sample was exposed to the suspension for 10 minutes. The three different shear rates examined were 9.55, 23.8, and 38.2 sec^{-1} and are designated as 0, ▽, and □ respectively.

Figure 5.2.1 illustrates that addition of red cells up to a hematocrit of 20% increases platelet adhesion to glass by a factor of 2 and that further increase in hematocrit does not alter the level of platelet adhesion. The fact that platelet surface density is independent of hematocrit above 20% is consistent with the hypothesis that the physical properties of red blood cells are responsible for increased platelet adhesion. This is explained by crowding of red blood cells at higher hematocrits, resulting in more multibody collisions and a reduction in red cell motions.

The rate of increase of platelet adhesion to collagen coated glass with hematocrit decreased at hematocrits greater than 20% (see Figures 5.2.2-5.2.3). At a hematocrit of 45%, platelet adhesion had fallen below the values associated with a 30% hematocrit and was not distinguishable from results obtained with a 15% hematocrit (see Figure 5.2.4).

The data of Figures 5.2.2 and 5.2.3 are cross plotted in Figures 5.2.5 and 5.2.6. At 0% hematocrit, platelet adhesion is independent of shear rate as expected from the fluid mechanics of a Couette flow device. The addition of red blood cells to the platelet suspension causes adhesion to be dependent on shear rate. This dependence suggests that platelet diffusivity, which is governed by the red blood cell motions induced by fluid shear, is a function of shear rate.

Some earlier experiments to determine if platelet diffusivity is a function of shear rate and hematocrit have proved inconclusive (16, 19). However, the Couette flow

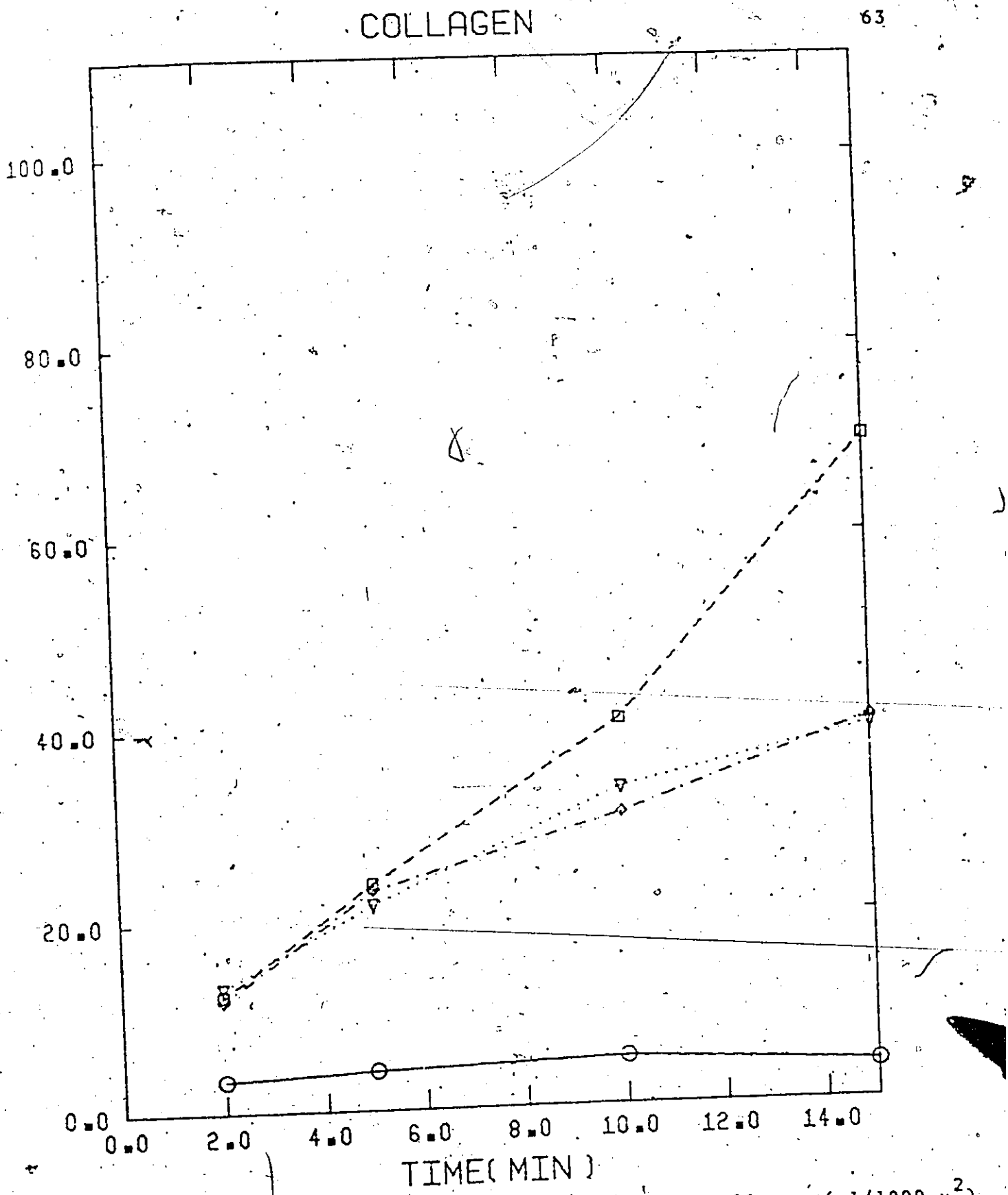

Figure 5.2.4. Plot of platelet surface density on collagen (pl/1000 μ^2) against time. Each point is the average of 2 observations and each sample was exposed to the suspension at a shear rate of 19 sec^{-1}. Four different hematocrits examined were 0%, 15%, 30% and 45% and are designated as 0, ▽, □ and ◇ respectively.

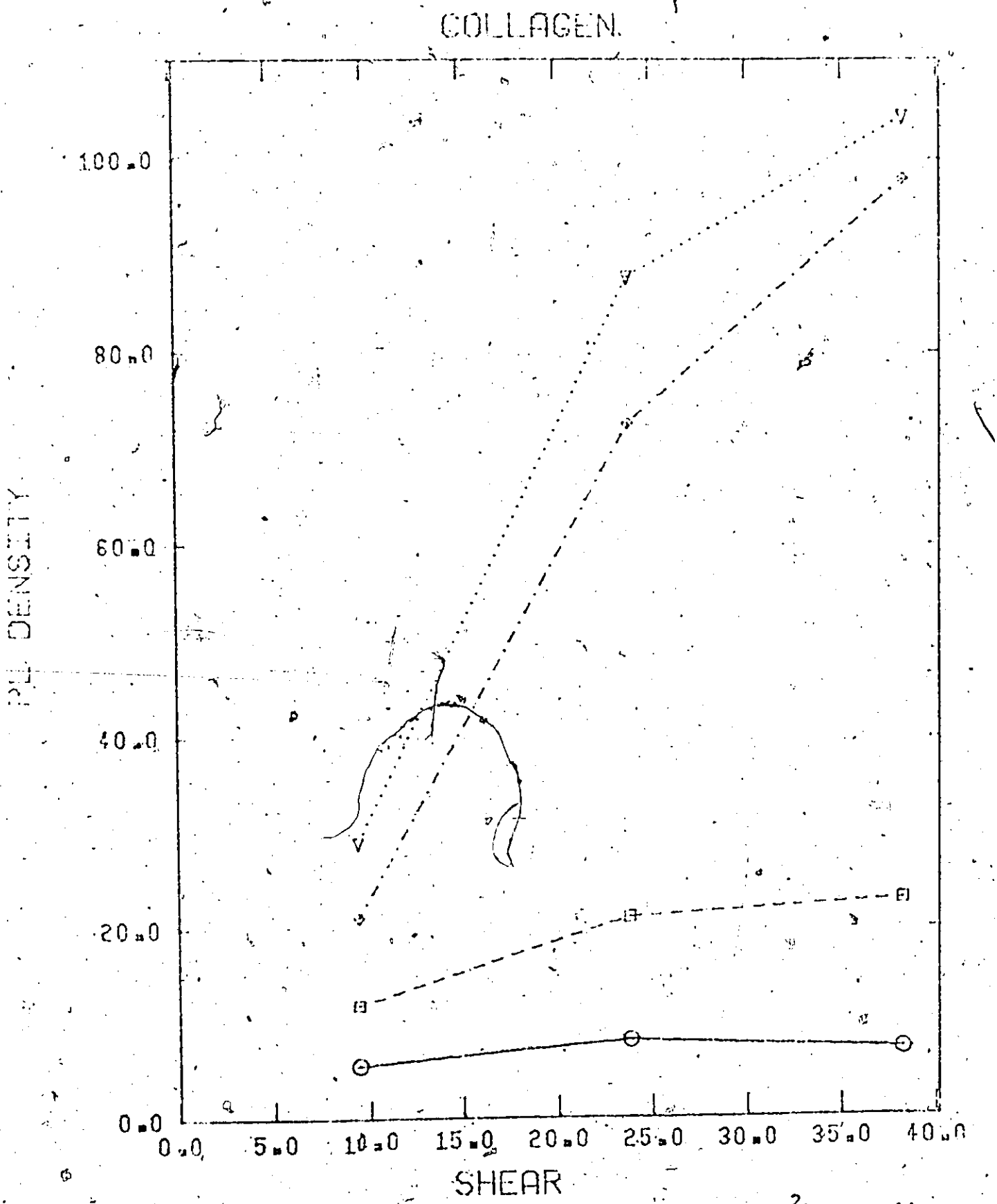

Figure 5.2.5. Plot of platelet surface density (pl/1000 μ^2) on collagen against shear rate. The four different hematocrits investigated were 0%, 5%, 20% and 30% and are designated as 0, □ , ◇ , and ▽ respectively. This is a cross plot of Figure 5.2.2.

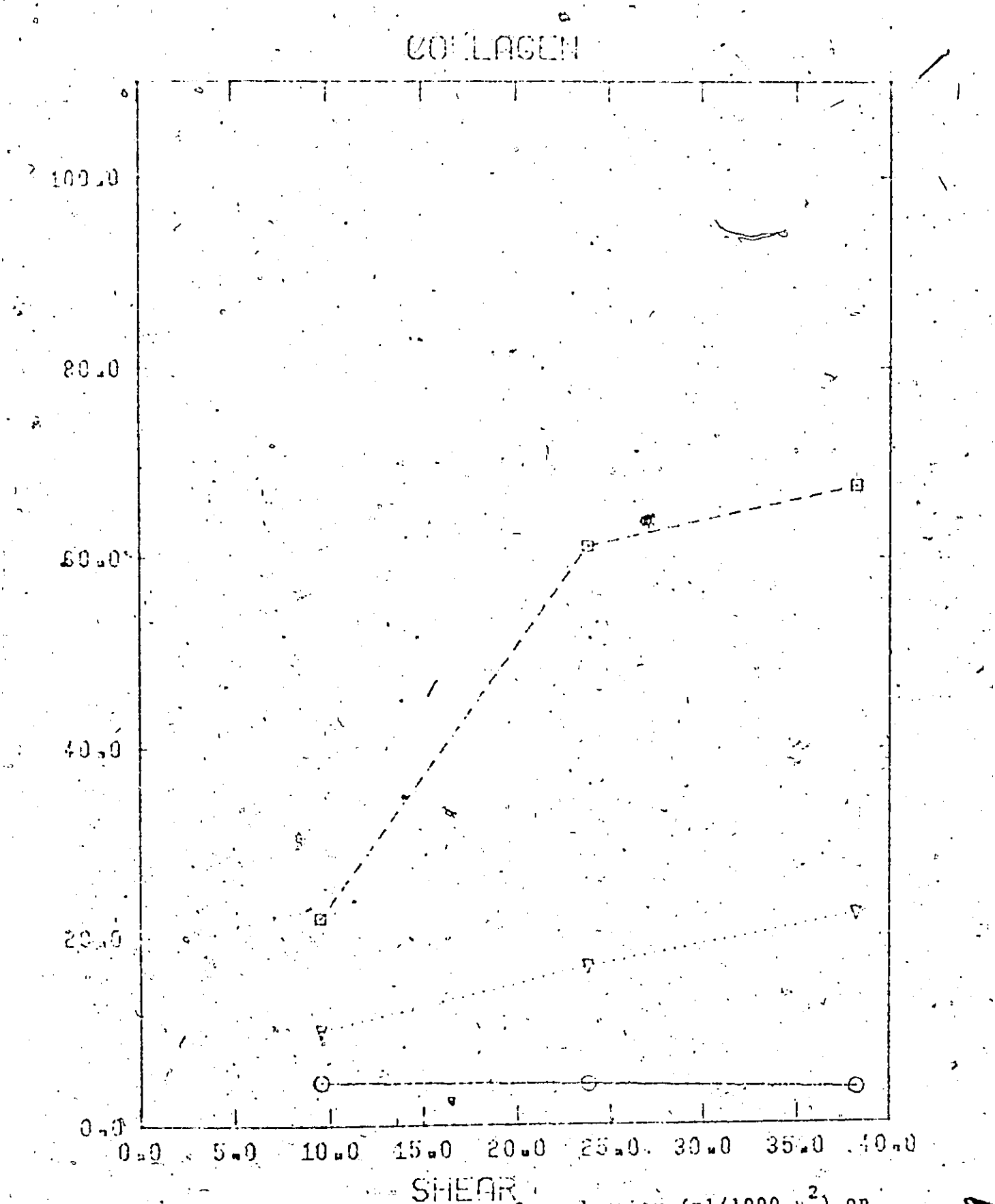

Figure 5.2.6. Plot of platelet surface density (pl/1000 μ^2) on collagen against shear rate. The three different hematocrits investigated were 0%, 5% and 30% and are designated as O, ▽, and □ respectively. This is a cross plot of Figure 5.2.3.

apparatus is especially suited to this task as there are no convective terms in the platelet mass balance equation describing flow in this device. The presence of increased levels of adhesion may then be attributed to platelet diffusivity being a function of shear rate.

The initial assumed model to express platelet diffusivity as a function of shear rate and hematocrit was given in Chapter 4 as

$$D_p = H^{\beta} \dot{\gamma}^{n} \qquad (4.17)$$

As we wish to quantify the relationship between shear rate, hematocrit and diffusivity, all experiments related to this question must be performed on the same day.

The best estimate of D_p is obtained from a nonlinear regression of Equation (4.10) and consequently to satisfy the implicit assumptions (diffusion limited mass transfer) in Equation (4.10) all rods were collagen coated. In order to provide the best estimate of D_p at a given shear rate and hematocrit, experiments should be performed at 2, 5, 10 and 15 minutes. The total duration of these experiments would be 32 minutes and in order that platelet damage due to fluid shear be eliminated, a fresh aliquot (70 ml.) of suspension would be required for each estimate of the diffusivity. To investigate diffusivities at the necessary number of different shear rates and hematocrits to obtain sufficient points to perform a regression of Equation (4.17) would require a volume of platelet suspension well in excess of the 200 ml. that we are

able to prepare daily. Because of these experimental limitations, diffusivities are calculated directly from Equation (4.10) at given conditions of hematocrit and shear rate.

Equation (4.17) predicts platelet diffusivity to be independent of shear rate at 0% hematocrit and this has been established experimentally as may be seen by referring to Figures 5.2.5 and 5.2.6.

Efficient estimates of β and n have been made by applying a logarithmic transformation of Equation (4.17) and then using linear least squares. This approach is justified since the residuals of the transformed equation will be shown to be independent and normally distributed with constant variances+. The regression analysis was performed on the data in Figures 5.2.2 and 5.2.3 using biomedical computer package BMD02R (82). The results of this regression are shown in Table 5.2.1.

Figure	β	S.D.	n	S.D.
5.2.7	1.48	.20	1.74	.27
5.2.8	1.16	.15	1.41	.24

Table 5.2.1. Effect of Shear Rate and Hematocrit on Platelet Diffusivity (Assumed Model $D_p = H^{\beta} \dot{\gamma}^{n}$)

The results of Table 5.2.1 appear to put the assumed diffusivity model in jeopardy. The shear rate dependence of

+ See Appendix C.

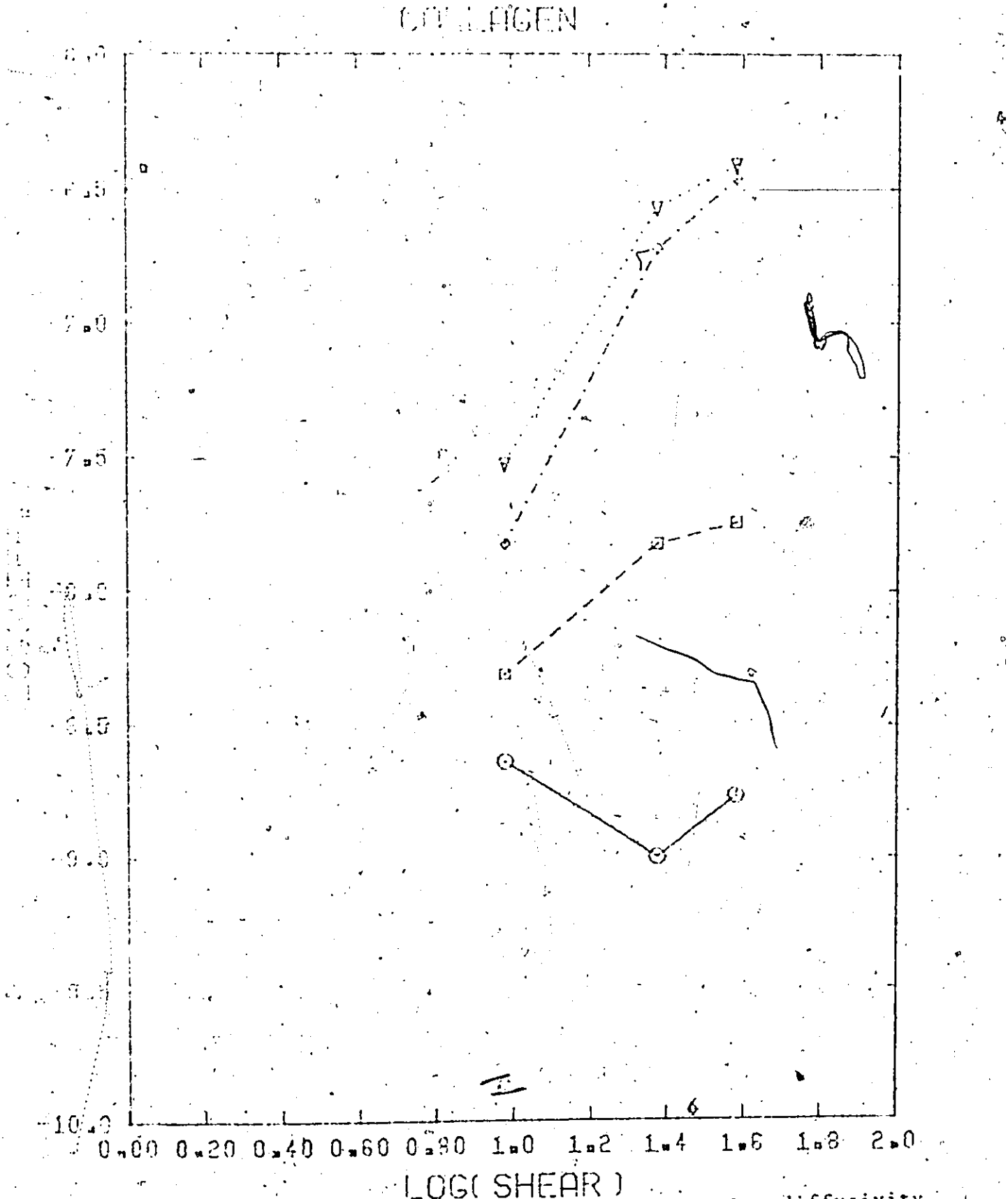

Figure 5.2.7. Logarithmic plot of calculated platelet diffusivity against shear rate. Each point is the average of two observations and is obtained under the experimental conditions of Figure 5.2.2. The four different curves represent hematocrits of 0% (O), 5% (□), 20% (◇) and 30%.

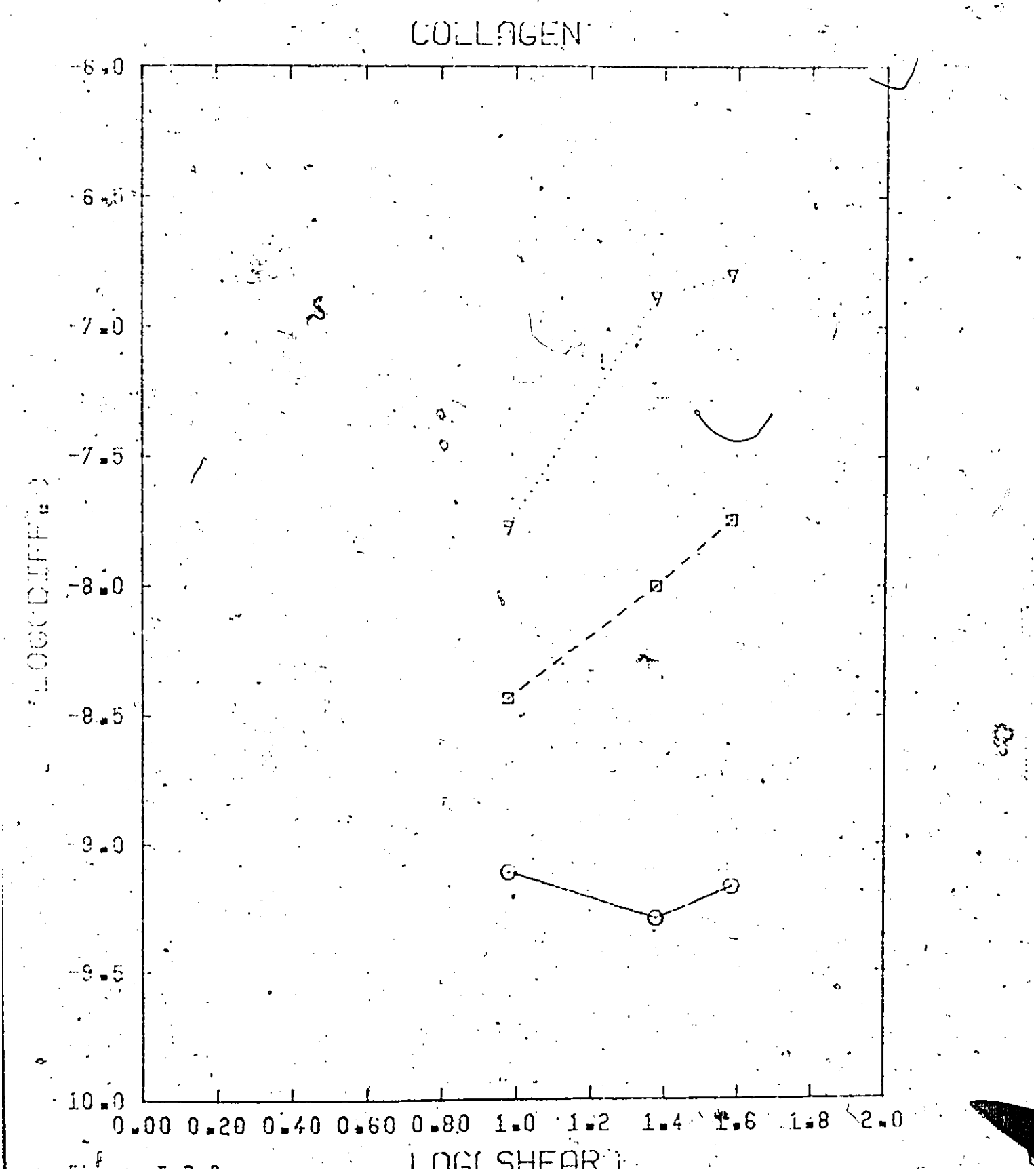

Figure 5.2.8. Logarithmic plot of calculated platelet diffusivity against shear rate. Each point is the average of two observations and is obtained under the exporimental conditions of Figure 5.2.3. The 3 different curves represent hematocrits of 0% (0), 5% (□) and 30% (▽).

platelet diffusivity is greater than one. This can not be interpreted physically as multibody collisons and crowding are expected to result in a shear rate dependence less than one (18).

Furthermore for constant hematocrit, Equation (4.17) predicts

$$\log (D_p) \alpha n \log \dot{\gamma} \qquad (5.1)$$

Table 5.2.2 shows the results of 4 regressions of $\log (D_p)$ and $\log \dot{\gamma}$ for different hematocrits. The results from this table illustrate that n is not a constant as originally assumed but is a function of hematocrit.

Hemat. (%)	n
0	.38
5	1.99
20	2.33
30	1.00

Table 5.2.2 Dependence of Shear Rate Exponent in the Diffusivity Model on Hematocrit*.

* Data obtained from Figure 5.2.2.

Since the motions of red cells are dependent on both the shear rate and the cellular concentration and in view of the data in Table 5.2.2, a more appropriate model for the

dependence of platelet diffusivity on shear rate and hematocrit might be given by

$$D = H^{\beta} \dot{\gamma}^{nH} \qquad (5.2)$$

A model of this form was regressed with the data from Figure 5.2.2. This regression gave a value of β not significantly different from zero and n equal to .06 with a standard error of 0.01. This model again predicts platelet diffusivity to be independent of shear rate at 0% hematocrit. The model predicts that the platelet diffusivity dependence on shear rate will increase with the addition of red cells. However, the model does not account for the decrease in red cell motions accompanying multibody collisions at high hematocrits (see Figure 5.2.4).

More experiments are needed to determine the exact functional form of the relationship between diffusivity, hematocrit and shear rate over a wide range of shear rates and hematocrits. However at low values of shear rate and hematocrit a model of the form

$$D \propto \dot{\gamma}^{nH} \qquad (5.3)$$

appears to describe the data.

5.3 Comparison with the Theoretical Model

Collagen is a very reactive surface with regard to platelet adhesion and does not appear to reach a saturation level before formation of a complete monolayer similar to

subendothelium (25, 83). Data for collagen coated glass in the early stages of adhesion should be represented by the diffusion controlled model which is expressed as

$$S = 2 C_o \left(\frac{D_p t}{\pi}\right)^{\frac{1}{2}} \qquad (4.10)$$

Equation (4.10) is nonlinear with respect to the diffusivity parameter. The program used to calculate the non-linear least squares estimate of the diffusivity operates on Marquardt's compromise between the method of steepest descent and Gaussian linearization (84). The residuals from the regression were independent and normally distributed with mean zero and a constant variance justifying the use of least squares.

Figure 5.3.1 is a plot of the surface platelet density on collagen coated glass on two different days. These experiments were run at 0% hematocrit and it is therefore expected that platelet diffusivity would be equal to the diffusivity predicted by Brownian motion. The results in Table 5.3.1 agree very well with the diffusivity of 1.4×10^{-9} $cm^2/sec.$ predicted by Brownian motion.

Day	Expected (Diffusivity)*	Confidence Intervals+
1	1.0×10^{-9}	$.8 \times 10^{-9}$ - 1.3×10^{-9}
2	$.9 \times 10^{-9}$	$.6 \times 10^{-9}$ - 1.1×10^{-9}

* Diffusivity Units ($cm^2/sec.$) + at 95%

Table 5.3.1 Estimates of Platelet Diffusivity at 0% Hematocrit.

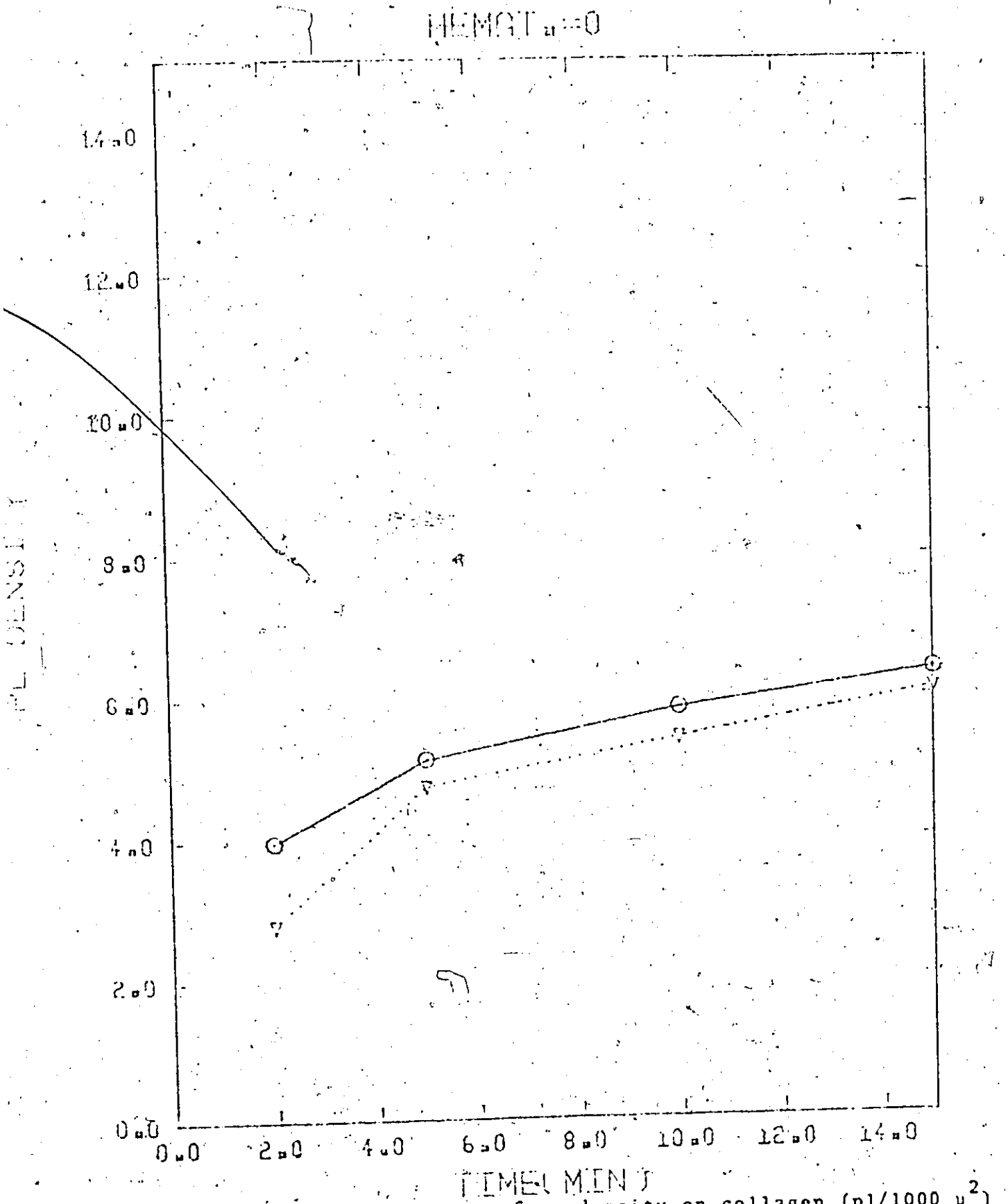

Figure 5.3.1. Plot of platelet surface density on collagen (pl/1000 μ^2) against time. Hematocrit = 0%. Each point is the average of 4 observations. Symbols: Day 1 - (0), Day 2 (▽).

Figures 5.3.2 - 5.3.4 show additional time studies of collagen coated glass in the presence of red cells. In all experiments the hematocrit was kept constant at 20% and the shear rate was 19 sec^{-1}. Table 5.3.2 shows the nonlinear least squares estimates of the diffusivities and the 95% confidence interval based on linear analysis of variance.

Figure	Expected (Diffusivity)*	Confidence Intervals	Date
5.2.2	1.1×10^{-7}	$.8 \times 10^{-7}$ - 1.4×10^{-7}	14/8
5.2.2	1.0×10^{-7}	$.82 \times 10^{-7}$ - 1.3×10^{-7}	16/8
5.2.2	$.60 \times 10^{-7}$	4.5×10^{-8} - 7.5×10^{-8}	20/8
5.2.3	$.51 \times 10^{-7}$	4.5×10^{-8} - 5.6×10^{-8}	20/6
5.2.3	$.82 \times 10^{-7}$	7.0×10^{-8} - 9.3×10^{-8}	21/6
5.2.4	$.42 \times 10^{-7}$	3.6×10^{-8} - 4.8×10^{-8}	24/7

*. Diffusivity Units ($cm^2/sec.$)

Table 5.3.2. Estimates of Platelet Diffusivity at 20% Hematocrit.

Three points should be made with regard to Table 5.3.2. First, the estimated diffusivities for each day are 10 - 100 times greater than the diffusivities predicted by Brownian motion. This is in agreement with the theory of an augmented platelet diffusivity due to the complex motions of the red blood cells. Secondly, the 95% confidence intervals are small indicating that the data is in good agreement with the diffusion

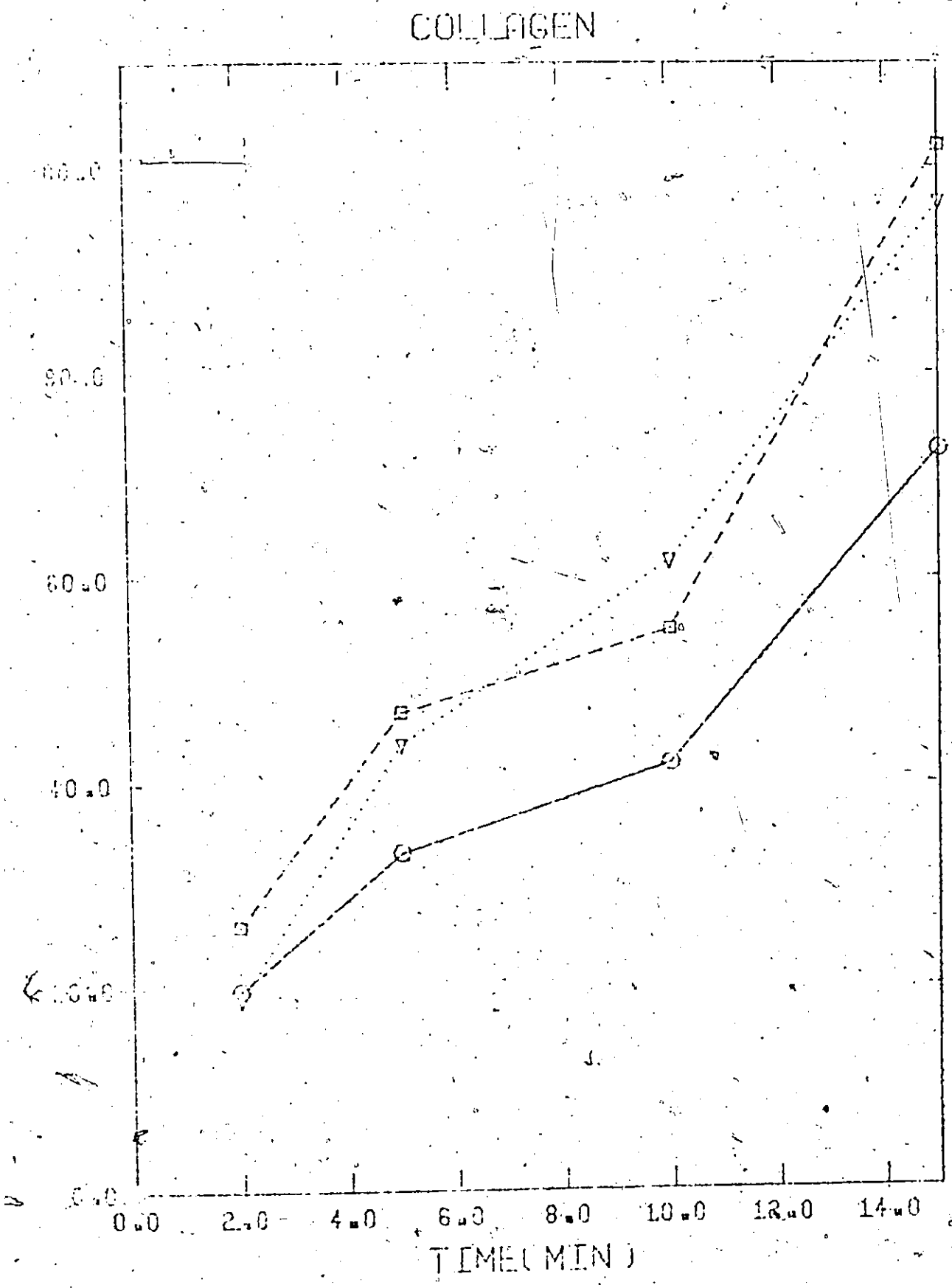

Figure 5.3.2. Plot of platelet surface density on collagen (pl/1000 μ^2) against time. Hematocrit = 20%. Each point is the average of 2 observations. Symbols: 20/8 (0), 16/8 (▽), 14/8 (□).

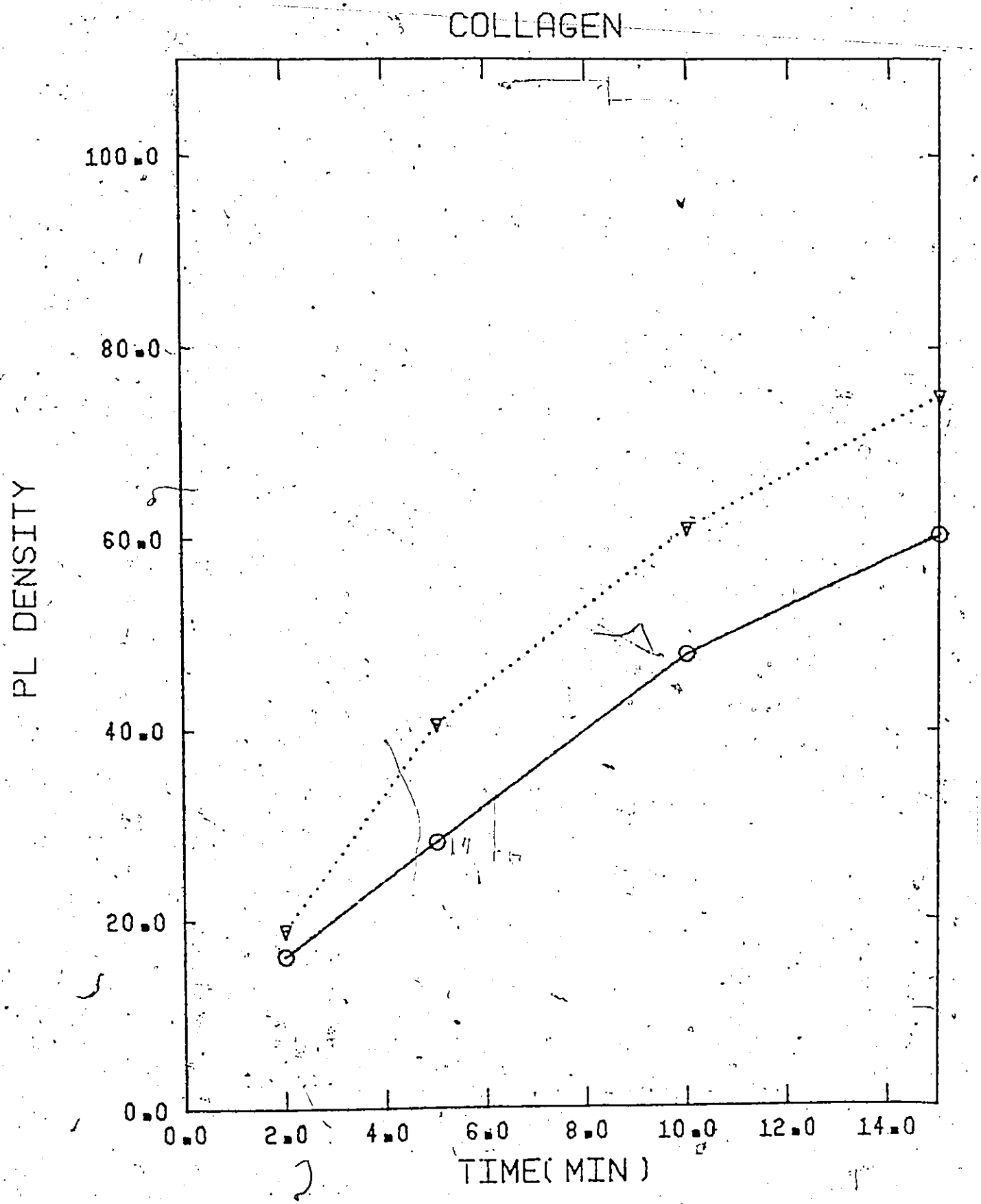

Figure 5.3.3. Plot of platelet surface density on collagen (pl/1000 μ^2) against time. Hematocrit = 20%. Each point for 20/6 (O) is the average of 4 observations. Each point for 21/6 (∇) is the average of 2 observations and the bulk platelet concentration for this day was 900,000 pl/mm^3.

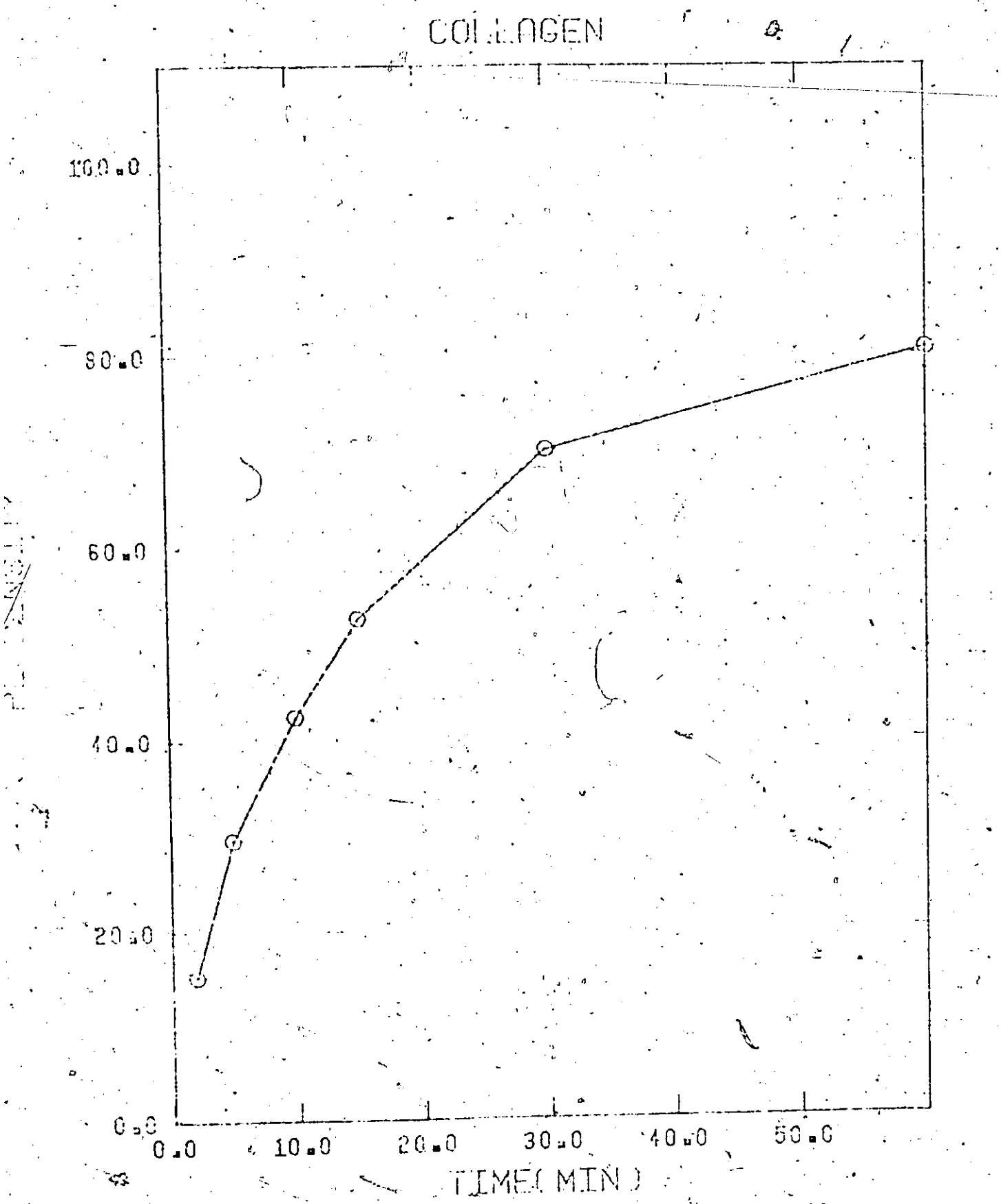

Figure 5.3.4. Plot of platelet surface density on collagen (pl/1000 μ^2) against time. Hematocrit = 20%. Each point is the avorage of two observations. Symbol: 24/7 - (0).

limited model. Finally, the differences from day to day are due to the daily platelet variability and make numerical comparisons uncertain.

A further indication of the validity of the diffusion limited model for platelet adhesion to collagen coated glass is illustrated in Figure 5.3.5. This shows that the platelet surface density varies approximately linearly with the platelet bulk concentration as predicted by Equation (4.10). The diffusion controlled model predicts a diffusivity of 10-100 times larger than the one due to Brownian motion alone and is in agreement with other investigators (2-6).

5.4 Effect of Different Surfaces

In the absence of red blood cells, low levels of platelet adhesion are observed on glass, polyurethane and collagen coated glass. This is illustrated by comparing Figure 5.4.1 and Figure 5.3.1. Both glass and collagen coated glass appear to reach an equilibrium value of between 2 and 5 platelets/1000 μ^2 in less than 2 minutes. Further, the levels of adhesion on the various surfaces are not statistically different at 50% confidence level. Again daily variations in platelet activity are visible.

The curves in Figure 5.3.1 and Figure 5.4.1 compare very well with the predicted values of platelet adhesion for the diffusion limited case using a diffusivity of 1.0×10^{-9} cm^2/sec) plotted in Figure 4.1.1 Since it has been established that collagen is more reactive than glass it appears that

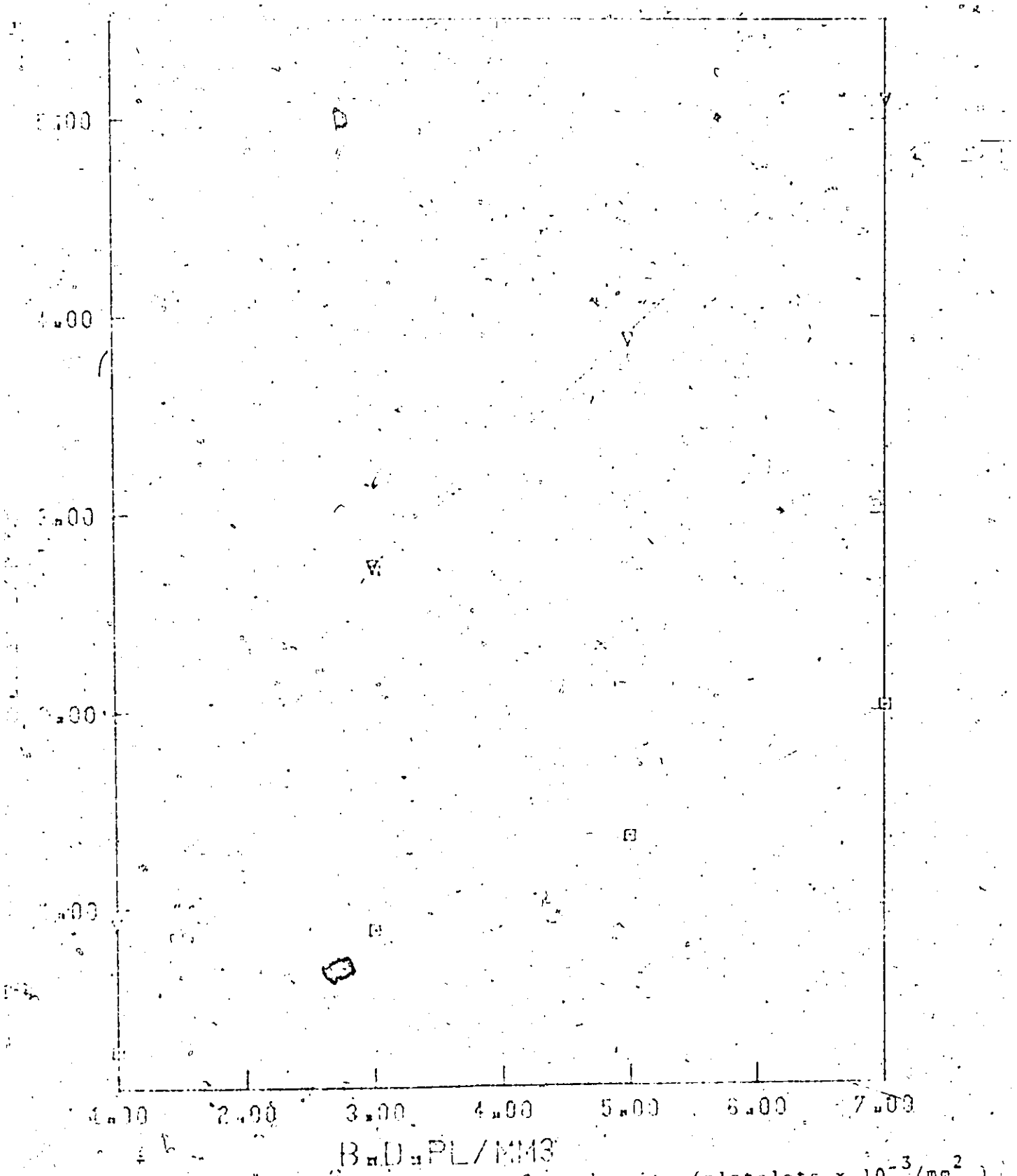

Figure 5.3.5. Plot of platelet surface density (platelets x $10^{-3}/mm^2$.) against platelet bulk concentration (platelets x $10^{-5}/mm^3$). Each point is the average of two observations. The hematocrit was 20%. Symbols: collagen coated glass exposed for 2 and 10 minutes respectively (□, ▽).

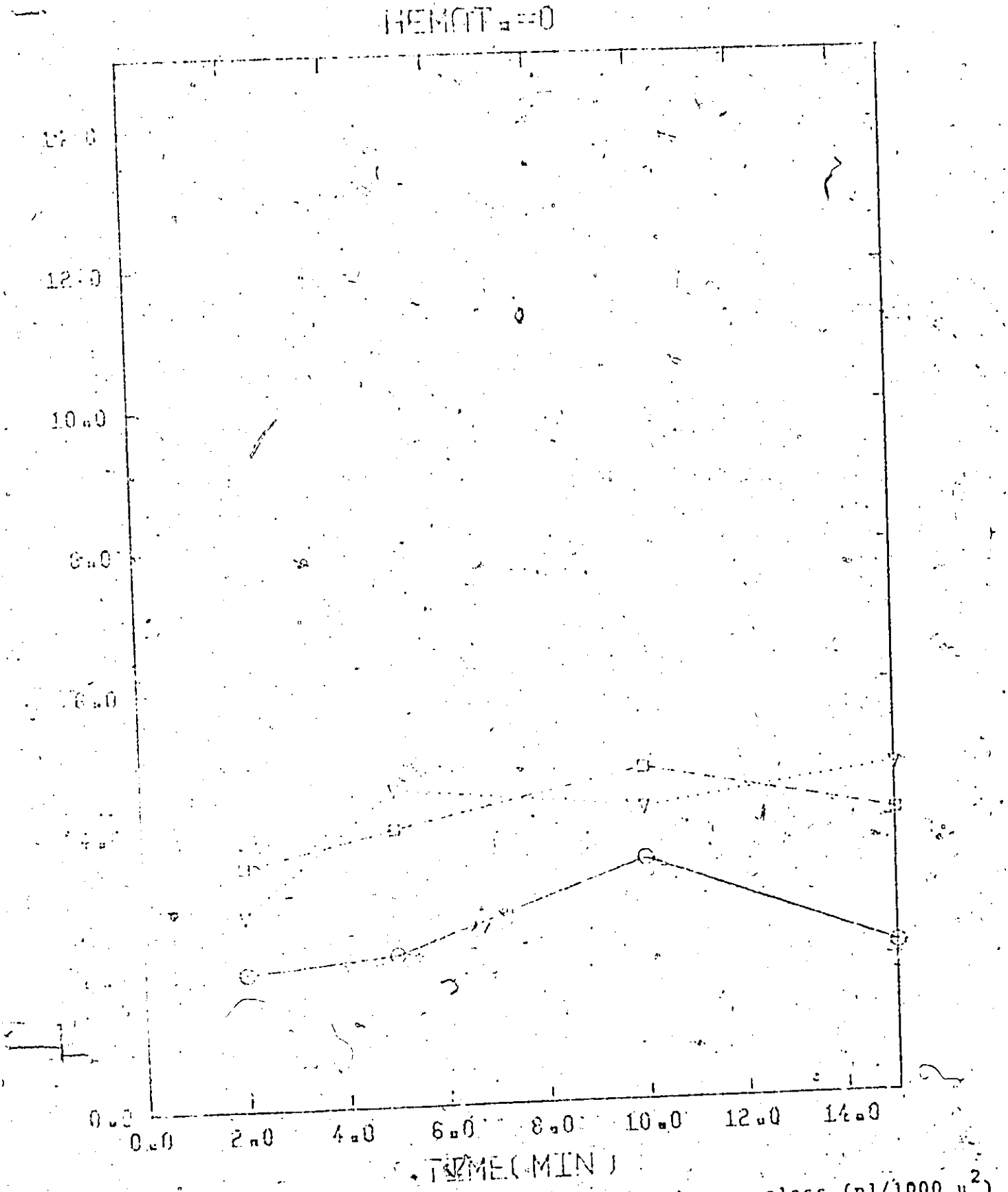

Figure 5.4.1. Plot of platelet surface density on glass (pl/1000 μ^2) against time. Each point is the average of four observations and each sample was exposed to a platelet suspension at a shear rate of 19 sec^{-1}. The three different curves represent experiments from three different days.

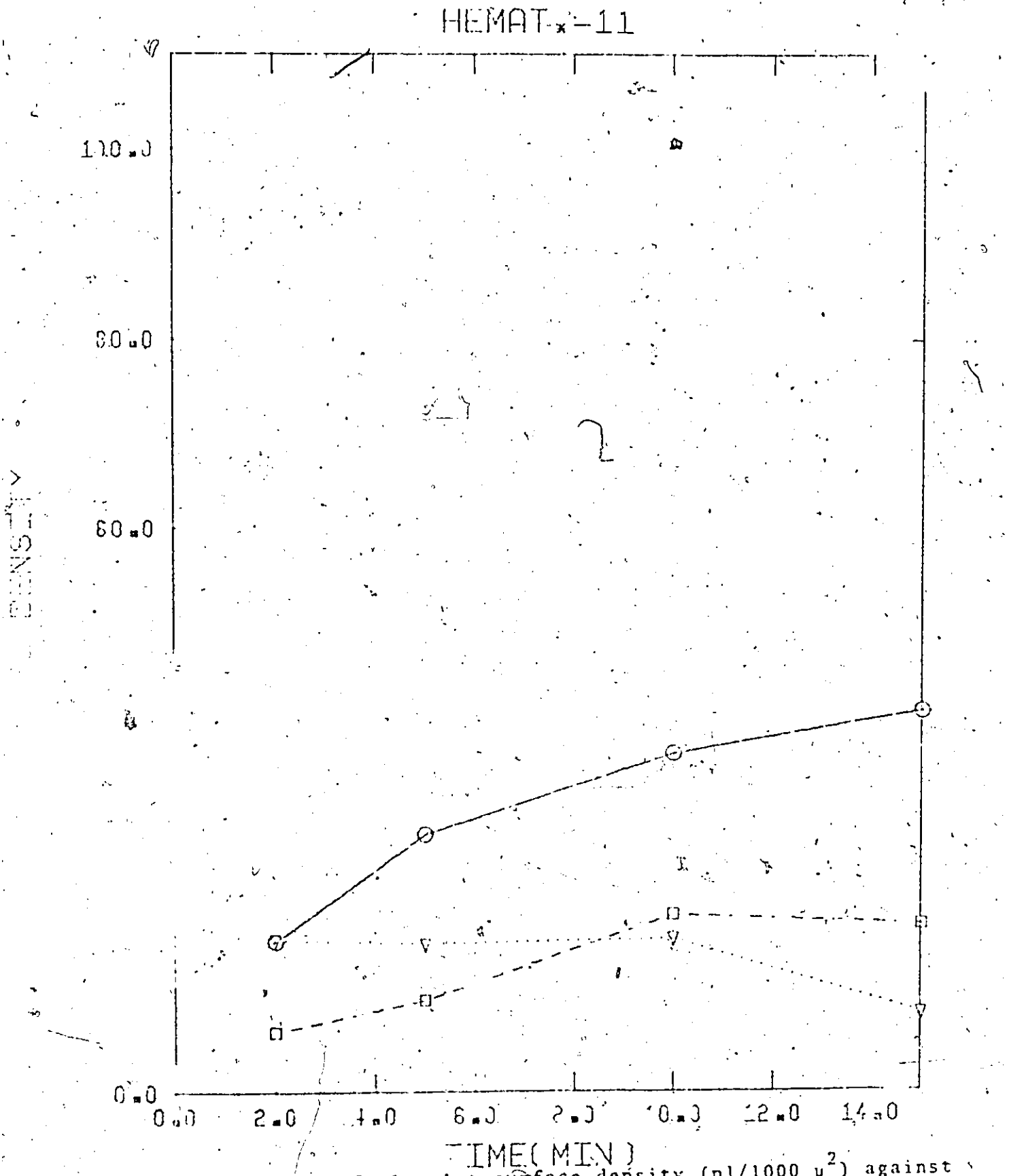

Figure 5.4.2. Plot of platelet surface density (pl/1000 μ^2) against time for various surfaces. Each point is the average of two observations. The homatocrit 11% and the shear rate 19 sec^{-1}. The three surfaces examined were collagen (O), glass (V) and polyurethane (□).

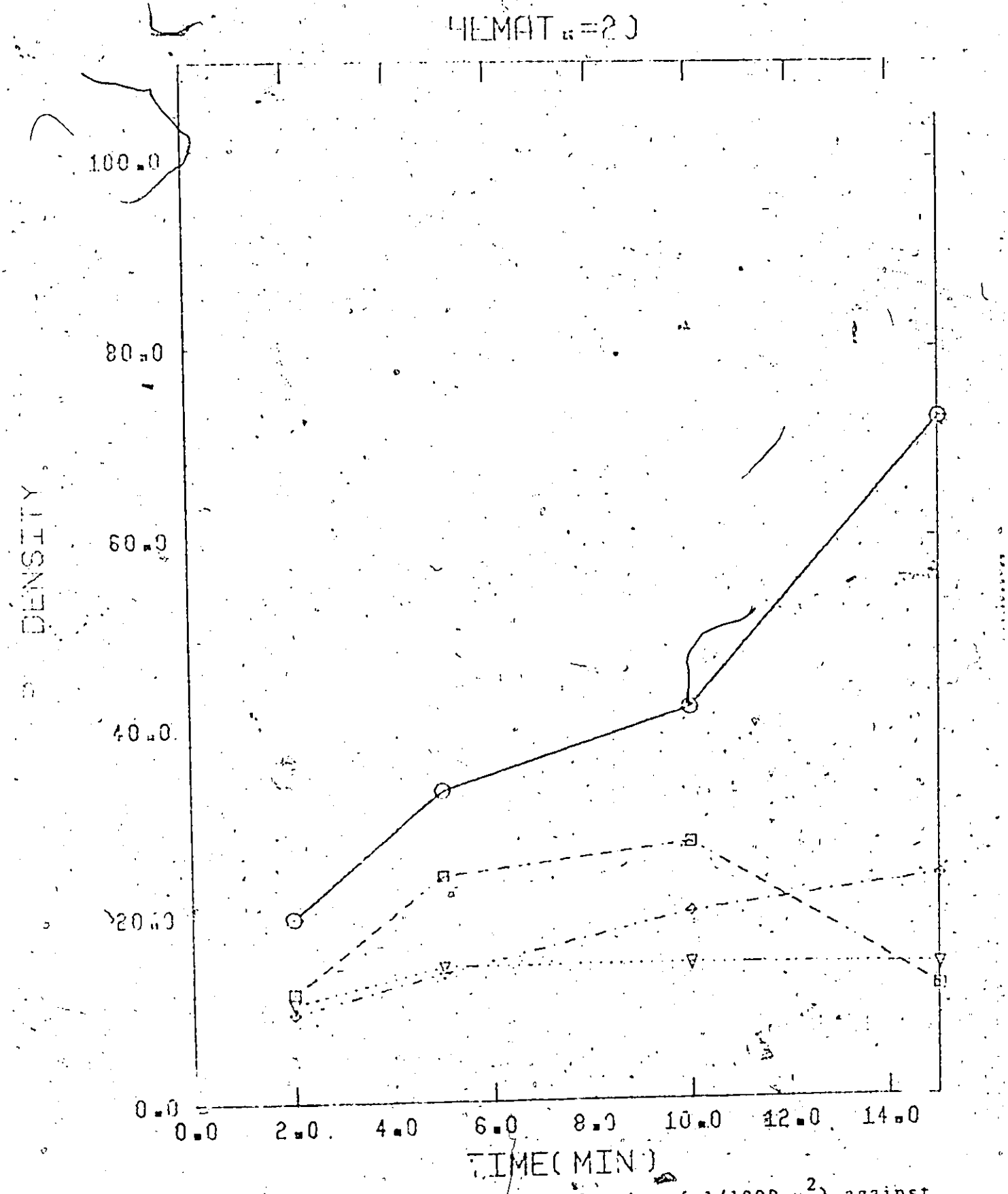

Figure 5.4.3. Plot of platelet surface density (pl/1000 μ^2) against time for various surfaces. Each point is the average of two observations. The hematocrit was 20% and the shear rate 19 sec^{-1}. The surfaces examined were collagen (○), glass (▽), polyurethane (□) and polystyrene (◇).

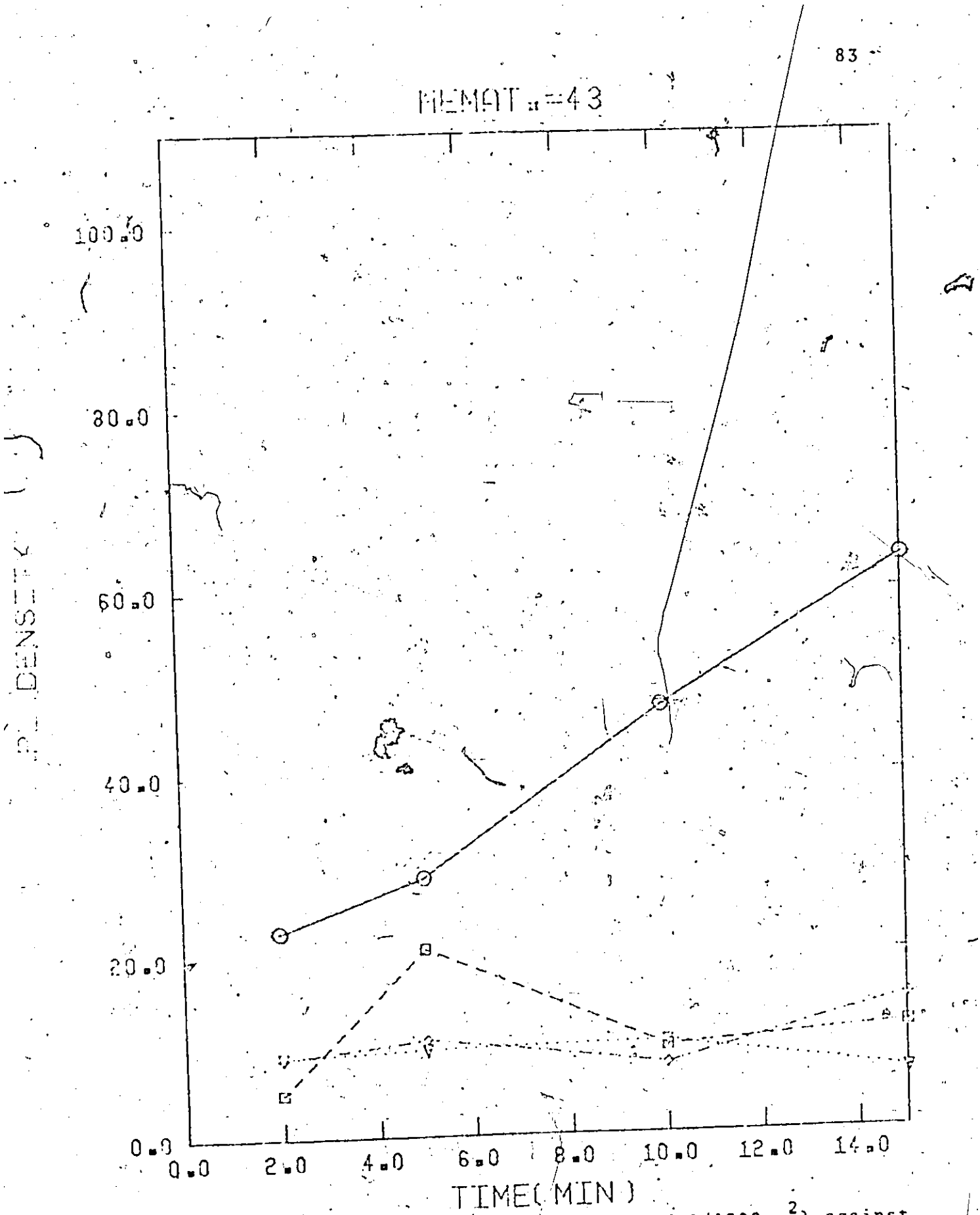

Figure 5.4.4. Plot of platelet surface density (pl/1000 μ^2) against time for various surfaces. Each point is the average of two observations. The hematocrit was 43% and the shear rate 19 sec^{-1}. The surfaces examined were collagen (O), glass (▽), polyurethane (◇), and polystyrene (□).

platelet adhesion is diffusion controlled at 0% hematocrit.

As shown in Figures 5.4.2-5.4.6 all surfaces studied in this work exhibit higher levels of platelet adhesion upon the addition of red blood cells. The elevated levels of adhesion could be explained in terms of increased energy of platelet-surface interaction caused by red cell motion.

In Figure 5.4.2 with an 11% hematocrit platelet adhesion on collagen is continually increasing with time and after 15 minutes the surface density is approximately 40 platelets/1000 μ^2. Glass appears to reach an equilibrium value of approximately 15 platelets/1000 μ^2 after an exposure time of 2 minutes. Polyurethane, after a period of about 10 minutes, has reached an equilibrium value not statistically different (at 95% confidence) from that of glass. The collagen data still appears to follow the diffusion limited model while the data for glass and polyurethane has reached a saturation value. For these two surfaces it appears that Equation (4.2) should be solved using the following boundary condition.

$$-D_p \frac{\partial c}{\partial x} = kcf \qquad (4.13)$$

where f is the fractional area not yet covered by platelets.

A solution for the differential equation (4.2) with Equation (4.13) has not been carried out as yet. A numerical solution is necessary due to the nonlinearity of boundary condition (4.13).

Increasing the hematocrit to 20%, Figure 5.4.3 did not alter the trends seen in Figure 5.4.2. The artificial surfaces including polystyrene as well as those studied previously again reach equilibrium values of between 15-25 platelets/1000 μ^2 and no statistically reliable differences can be reported. The level of adhesion to collagen coated glass in Figure 5.4.3 has increased over that of Figure 5.4.2. We cannot distinguish between the possibilities that this increase is due to the increase in hematocrit or to the daily variations in platelet activity.

The data presented in Figure 5.4.4 were obtained with an approximately physiological hematocrit of 43%. The overall trends are again consistent with the data for different surfaces generated at 11% and 20%. Preliminary investigation of 4 different surfaces thus shows that platelet adhesion to these surfaces does not vary as the red cell concentration varies from 11% to 43%.

The artificial surfaces reach an equilibrium value after less than 10 minutes exposure. In most cases, the equilibrium value has been reached in 2 minutes. Friedman et al. (16) reported that platelet adhesion levelled off at approximately 20 minutes and was independent of the surface involved. In our experiments glass, polyurethane, polystyrene and sulphonated polystyrene all equilibrated at 15-25 pl/1000 μ^2.

Figures 5.4.5 and 5.4.6 illustrate that albumin coated glass reaches a much lower equilibrium value than the other surfaces. The equilibrium value is reached in less than 2,

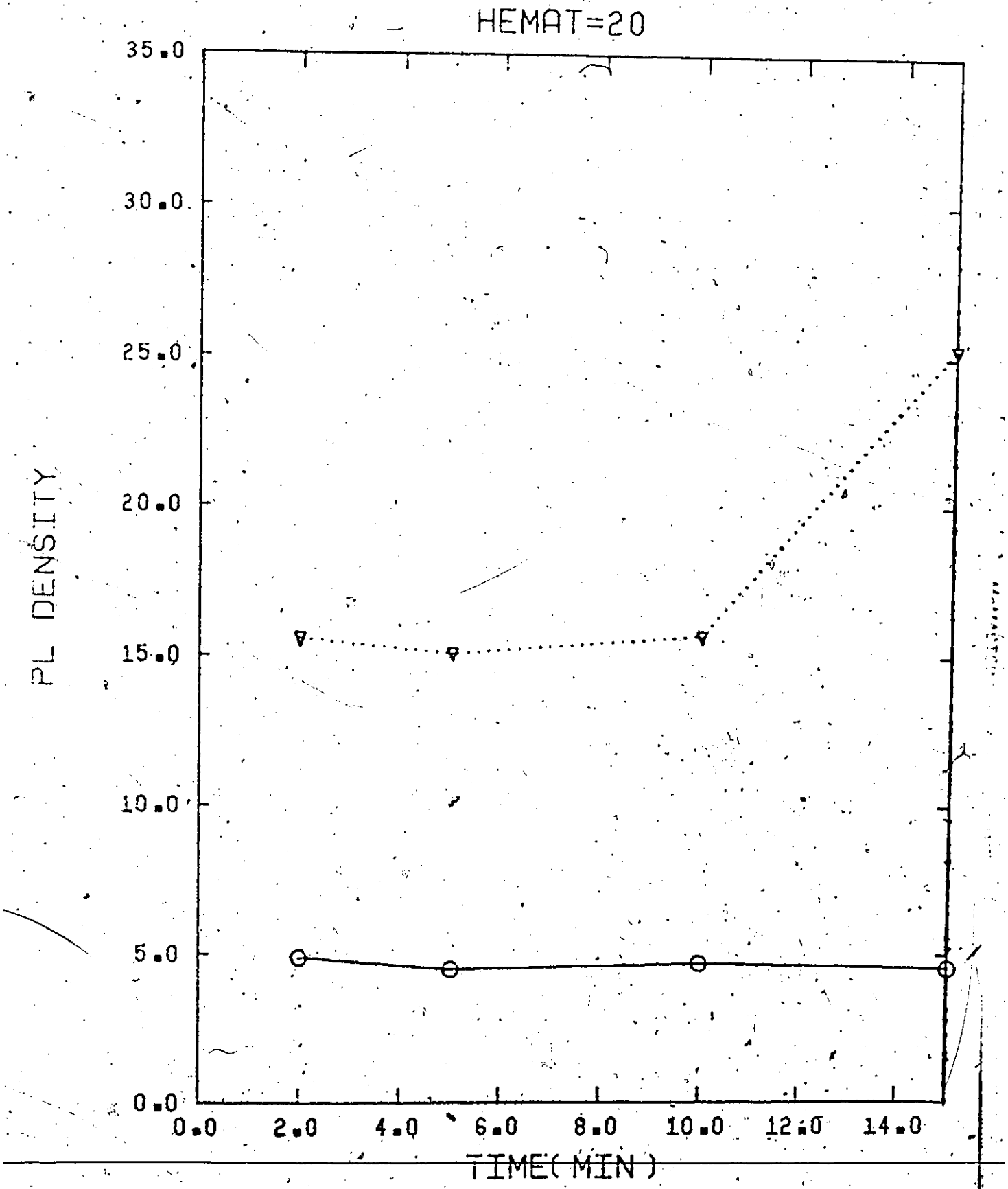

Figure 5.4.5. Plot of platelet surface density (pl/1000 μ^2) against time for two surfaces. Each point is the average of two observations. The hematocrit was 20% and the shear rate 19 sec^{-1}. The surfaces examined were glass (▽) and albumin coated glass (○).

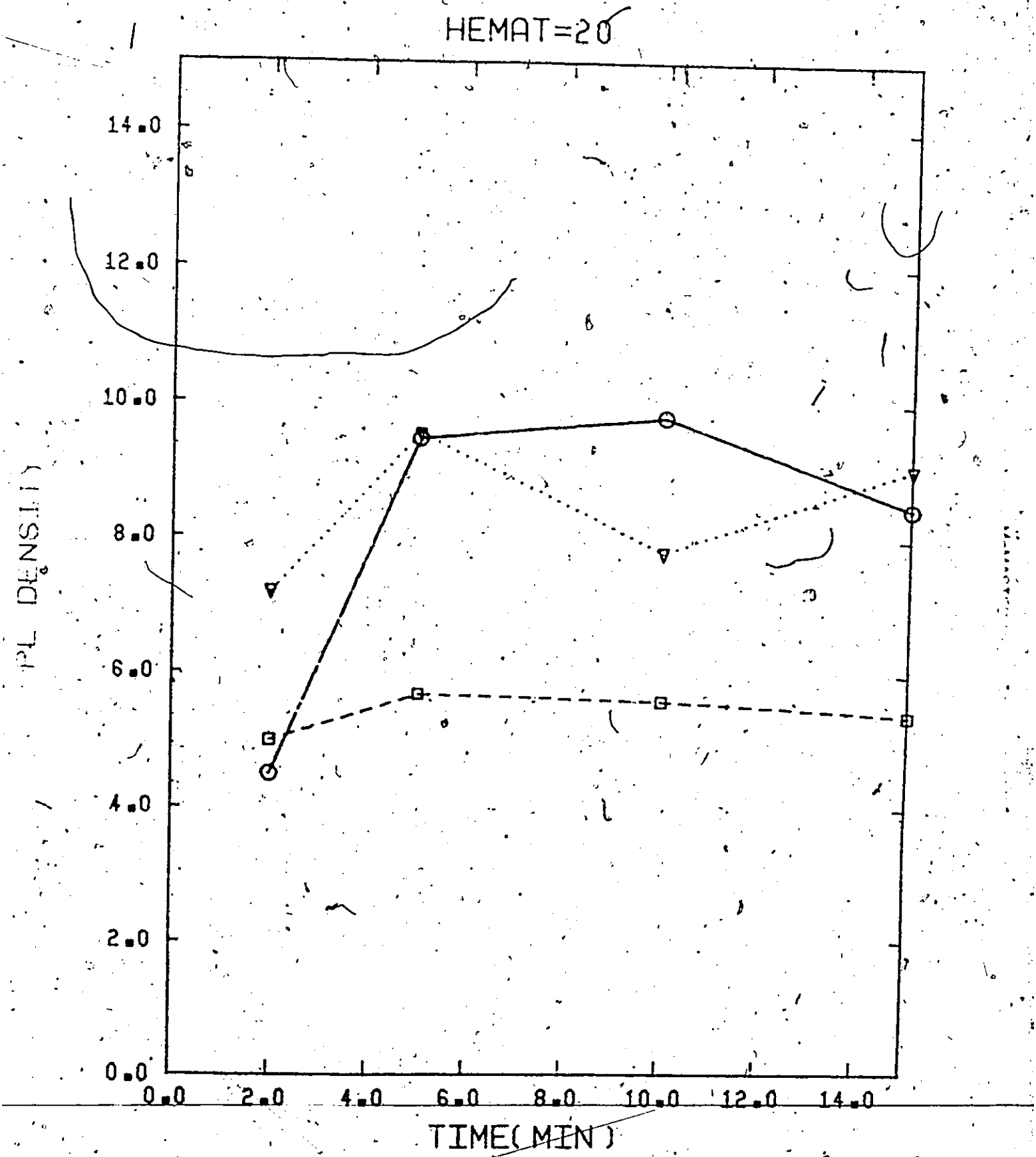

Figure 5.4.6. Plot of platelet surface density (pl/1000 μ^2) against time for 3 surfaces. Each point is the average of two observations. The hematocrit was 20% and the shear rate 19 sec^{-1}. The surfaces examined were polyurethane (▽), polystyrene (○) and albumin coated glass (□).

minutes. Albumin has been reported elsewhere to inhibit platelet adhesion (58, 64).

In conclusion, it appears that platelet adhesion to collagen follows a diffusion limited process while the other surfaces investigated are characterized by the additional parameter of surface kinetics with the presence of saturation effects.

CHAPTER 6

SUMMARY AND CONCLUSIONS

The purpose of this work has been to develop an experimental flow system which will allow the thromboresistance of various biomaterials to be examined under well defined flow conditions and with well defined biological media. The thromboresistance has been evaluated by measuring the adhesion levels of radioactive labelled platelets.

Electron micrographs have revealed that fibrinogen is not necessary for the adhesion of pig platelets and that the radioactive counting procedure is valid. The effect of the parameters, time, shear rate, hematocrit, temperature and bulk platelet concentration on platelet adhesion have been investigated. A standard operating procedure has also been defined and the experimental device is designed to operate under Couette flow conditions.

A theoretical model, based on the continuum theory of mass transport, has been developed for the adhesion of platelets to highly reactive materials in the absence of saturation effects. Collagen has these appropriate properties and the model is referred to as diffusion limited. Using the experimental data for collagen coated glass in platelet suspensions (0% hematocrit) the theoretical model predicts a platelet diffusivity very close to the one based on Brownian motion. Different surfaces exhibit similar levels of platelet adhesion

when red blood cells are not present.

The addition of red cells has been found to increase platelet diffusivity by a factor of 10-100 resulting in close agreement with previous investigators (2-6). Furthermore, there are indications that the platelet diffusivity is a function of hematocrit and shear rate.

A theoretical model has not been presented for the other artificial surfaces because of a nonlinear boundary condition associated with the saturation effects that these surfaces exhibit. All the artificial surfaces seem to reach their equilibrium value after less than 10 minute exposures. Glass, hydrophobic polyurethane, polystyrene and sulphonated polystyrene all equilibrate at approximately the same value of platelet adhesion. Platelet adhesion on albumin coated glass is greatly reduced and this difference in adhesion levels from the other surfaces suggests that both platelet and surface reactivity are important in platelet adhesion to these artificial surfaces in the presence of red blood cells.

The excellent agreement of the calculated diffusivities with the predicted values, the high and low levels of platelet adhesion to collagen coated glass and albumin coated glass respectively and the enhanced platelet diffusivity due to the presence of red cells as predicted in the literature indicate a reliable experimental design. The differences in platelet adhesion to glass, collagen coated glass and albumin coated glass suggests that the equipment may be satisfactorily employed to evaluate platelet adhesion on other surfaces under well

defined fluid flow.

Presently, work is being carried out in this laboratory to investigate the interactions between plasma proteins and artificial surfaces. The platelet suspension preparation is flexible enough to allow intlusion of any proteins that are considered important in platelet adhesion and thrombus formation. The integration of the plasma protein work with the experimental work on platelet adhesion should further elucidate the mechanisms of platelet adhesion and assist in evaluating the blood compatibility of materials.

LITERATURE CITED.

1. Goldsmith, H. L., Progress in Hemostasis and Thrombosis, p. 97, T.H. Spaet, (ed.), Grane and Stratton, New York, (1972).

2. Goldsmith, H. L., Fed. Proc., 30, 1578 (1971).

3. Meiselman, H. G., Goldsmith, H. L., Thromb. Diath. Haemorsh., Suppl., 54, 273 (1973).

4. Keller, K. H., Fed. Proc., 30, 1591 (1971).

5. Bernstein, E. F., Blackshear, P. L., Keller, K. H., Am. J. Surg., 114, 126, (1967).

6. Blackshear, P. L., Dorman, F. D., Steinback, J. H., Trans. Amer. Soc. Artif. Int. Organs, 12, 112 (1965).

7. Meiselman, H. J., E. W. Merrill, Bibl. Anat., 9, 238 (1967).

8. Burton, A. C., Physiology and Biophysics of the Circulation, p. 45, Medical Year Book Publishers (1972).

9. Cokelet, G. R., Biomechanics, its Foundations and Objectives, p. 63, Y. C. Fung (ed.), Prentice-Hall, N.J. (1972).

10. Copely, A. L., Proc. 5th Int. Cong. on Rheology, p. 3, Vol. 2, Onogi (ed.), Baltimore Univ. Book Press (1970).

11. Rahn, E., Chemical Engineering in Biology, p. 45, Hershey (ed.), New York (1967).

12. Segre, G., Silberberg, J., J. Fluid Mech., 14; 136 (1962).

13. Blackshear, P. L., Forstorm, R. J., Dormen, F. D., Voss, G. O., Fed. Proc., 30, 1600 (1971).

14. Goldsmith, H. L., Mason, I. G., Proc. Roy. Soc. (London), 282, 589 (1964).

15. Bugliasello, G., Biomaterials, Stark, L., and Aganval, G. (ed.), p. 131, Plenum (1969).

16. Friedman, L. I., Lein, H., Grabowski, E. P., Leonard, E. F., McCord, C. W., Amer. Soc. Artif. Int. Organs, 16, 63 (1970).

17. Graboski, E. F., Ph.D. Thesis, Columbia University (1972).

18. Grabowski, E. F., Friedman, L. I., Leonard, E. F., 2nd Eng. Chem. Fundamentals, 11, 224 (1972).

19. Turitto, V. T., Leonard, E. F., Trans. Amer. Soc. Artif. Int. Organs, 18, 348 (1972).

20. Johnson, S. A., Blood Clotting Enzymology, p. 379, Seegers, W. H. (ed.), Academic Press, N.Y. (1967).

21. Baier, R. E., Dutton, R. C., J. Biomed. Mat. Res., 3, 191 (1969).

22. Dutton, R. E., Webber, A. J., Johnson, S. A., Baier, R. E., J. Biomed. Mater. Res., 3, 13 (1969).

23. George, J. N., Blood, 40, 862 (1972).

24. Brinkhaus, K. M., Fed. Proc., 26, 84 (1967).

25. Baumgartner, H. R., Micro. Res., 5, 167 (1973).

26. Baumgartner, H. R., Ann., N.Y., 201, 22 (1972).

27. Seeger, W. H., Blood Clotting Enzymology, p. 1, Seegers, W. H. (ed.), Academic Press, N.Y. (1967).

28. Vroman, L. Blood Clotting Enzymology, p. 279, Seegers, W. H. (ed.), Academic Press, N.Y. (1967).

29. Leonard, E. F., Friedman, L. I., Chem. Eng. Prog. Symp. Series, 66, 60 (1970).

30. Marcus, A. J., Thromb. Diath. Haemorrhag., Suppl. 17, 85 (1965).

31. Mustard, J. F., Rowsell, H. C., Murphy, E. A., Brit. J. Haematol, 12, 1 (1966).

32. Mustard, J. F., Packman, M. A., Pharm. Review, 22, 97 (1970).

33. Zucker, M. B., Borrelli, J., J. Appl. Physiol., 7, 425 (1955).

34. Gaardner, A., Jonsen, J., Laland, S., Hellem, A. J., Owren, P. A., Nature (London), 192, 531 (1961).

35. Mitchell, J. R. A., Sharp, A. A., Brit. J. Haematol, 10, 78 (1964).

36. Caen, J., Castaldi, P., Inceman, S., Nouvelle Rev. Franc. Hematol., 5, 327 (1965).

37. Lambert, H., Die Physikalische Seite des Blutgerinnings. Problems, George Thieme, Leipsig (A31).

38.

39. Copely, A. L., Glover, F. A., Scott-Blair, G. W., Biorheology, 2, 29 (1964).

40. Gayton, A. C., Basic Human Physiology, Saunders, Philadelphia (1971).

41. Weiss, Exp., Cell. Res., 53, 603 (1968).

42. Leonard, E. F., Trans. Amer. Soc. Artif. Int. Organs, 15, 15 (1969).

43. Murphy, P. et al., Trans. Amer. Soc. Artif. Int. Organs, 13, 131 (1967).

44. Lee, Neville, Handbook of Biomedical Plastics, 3-23, Pasadena Press (1971).

45. Levowitz, B. S., LaGuerre, J. N., Calem, W. S. Gould, F. E., Schorrer, J., Schoenfeld, Trand. Am. Soc. Artif. Int. Organs, 14, 82 (1968).

46. Hoffman, A. S., Schner, G., Harris, C., Kraft, W. G., Trans. Amer. Soc. Artif. Int. Organs, 18, 10 (1972).

47. Brash, J. L., Fritzinger, B. K., and Loo, B. H., Report No PB 197, 352, to National Heart and Lung Institute, Oct., 1974.

48. Brash, J. L. Fritzinger, and Loo, B. H., Report No. PB 210, 665, to National Heart and Lung Institute, April, 1972.

49. Lyman, D. J., Muir, W. M., Lee, I. J., Trans. Amer. Soc. Artif. Int. Organs, XI, 301 (1965).

50. Lyman, D. J., Brash, J. L. Chaikin, S. W., Klein, K. G., Carni, H., Trans. Amer. Soc. Artif. Int. Organs, 14, 250 (1968).

51. Lyman, D. J., Klein, K. G., Brash, J. L., Fritzinger, B. K., Thromb. Diath. Haemorrhagica, 23, 120 (1968).

52. Hellen, A. J., Scand. J. Clin. Lab. Invest., 12, Suppl. 51, (1960).

53. Glynn, M. F., Movat, H. Z., Murphy, E. A., Mustard, J.F., J. Lab. Clinic Med., 65, 179 (1965).

54. Mustard, J. F., Clynn, M. F., Nishizawa, E. E., Packman, M. A., Fed. Proc., 26, 106 (1967).

55. Bowie, J. W., Owen, C. A., Am. J. Clin. Path., 56, 479 (1971).

56. Cazenave, J. P., Packman, M. A., Guccionne, M. A., Mustard, J.F., Proc. Soc. Exp. Biol. Med., 142, 159 (1973).

57. Cazenave, J. P., Packman, M. A., Guccione, M. A., Mustard, J.F., J. Lab. Clin. Med., 83, 797 (1974).

58. Cazenave, J. P., Packman, M. A., Mustard, J.F., J. Lab. Clin. Med., 82, 978 (1973).

59. Wright, H. P. J. Path. Bact., 53, 255 (1941).

60. Hirsh, J., McBride, J. A., Wright, H. P., Thromb. Diath. Haemorrh., 16, 100 (1966).

61. Petschek, H. E., Adanis, D., Kantrowitz, A. R., Trans. Am. Soc. Artif. Int. Organs, 14, 256 (1968).

62. Dutton, R. C. Baier, R. E., Bedrick, R. L., Bowman, R. C., Trans. Am. Soc. Artif. Int. Organs, 14, 57 (1968).

63. Murphy, E. A., Roswell, H. C., Downie, H. G., Robinson, G.A., Mustard, J.F., Can. Med. Assoc. J., 87, 259 (1962).

64. Chang, T. M. S., Can. J. Physio. Phar., 52, 275 (1974).

65. Taylor, G. I., Phil. Trans. A., 223, 239 (1922).

66. Schlichting, H., Boundary Layer Theory, 6th edition, McGraw-Hill, New York (1968).

67. Tsukada, T., Steiner, M., Baldini, M., Am. J. Physio, 221, 1697 (1971).

68. Kattloue, H. E., Spaet, T. H., Blood, 35, 659 (1970).

69. Tsukada, T., Steiner, M., Baldini, M., Scand. J. Haematol., 8, 270 (1971).

70. Cazenave, J.P., Personal Communication.

71. Aster, R. H., Platelet Kinetics, p. 3, Paulus (ed.), Elsevier, New York (1971).

72. Born, G. V. R., Cross, M. J., J. Physiol. (London), 170, 397 (1964).

73. McLean, J. R., Maxwell, R. E., Hertler, D., Nature (London), 202, 605 (1964).

74. Baumgartner, H. R., Proc. 4th Cong. Int. Soc. Thrombo. Haemo., Vienna, Austria, p. 42 (1973).

75. Brash, J. L., Fritzinger, B. K., Bruch, D. S., J. Biomed. Mater. Res., 7, 313 (1973).

76. Brash, J., Dept. of Chemical Engineering, McMaster University, Hamilton.

77. Hamielec, A., Dept. of Chemical Engineering, McMaster University, Hamilton.

78. Himmelblau, D., M., Process Analysis by Statistical Methods, p. 24, John Wiley (1960).

79. Bird, R. B., Stewart, W. E., Lightfoot, E. N., Transport Phenomena, John Wiley (1960).

80. Carslaw, H. S., Jaeger, J. C., Conduction of Heat in Solids, Clarendon Press, Oxford (1959).

81. Crank, J., Mathematics of Diffusion, University Press, Oxford, p. 35 (1970).

82. Dixon, W. J. (ed.), Biomedical Computer Programs, Univ. of Calif. Press, Berkeley (1971).

83. Allen, D. J., Personal Communication.

84. UWHAUS, Nonlinear Least Squares Program, University of Wisconsin.

APPENDIX A

PREPARATION OF STOCK SOLUTIONS

The Tyrodes Albumin suspending medium is prepared by adding 5 ml. of stock solution #1, 1 ml. of stock solution #2, 2 ml. of stock solution #3, .35 gm. of bovine albumin and .1 gm. dextrose to 92 ml. of distilled water. Next the pH is adjusted to 7.35 and .6 ml. of 30% NaCl is added to produce the appropriate osmolarity. The composition of the stock solutions are as follows.

Stock Solution #1:

NaCl	160 gm.
KCl	4 gm.
$NaHCO_3$	20 gm.
NaH_2PO_4	1 gm.

Make up to 1.0 liter with deionized distilled water.

Stock Solution #2:

10^{-1} m. $MgCl_2.6\ H_2O$ 20.33 gm.

Dissolve in 900 mls. of dimineralized water. Bring to a total volume of 1.0 liter.

Stock Solution #3:

10^{-1} m. $CaCl_2 \cdot 6H_2O$ 21.91 gm.

Dissolve in 900 mls. of demineralized water and bring up to a total volume of 1.0 liter.

The plain Tyrodes solution is prepared by diluting 50 ml. of stock solution #1 with 950 ml. deionized distilled water.

The Tris buffer solution is prepared by adding 500 ml. of 0.2 m. Tris (hydroxymethyl) aminomethane, 414 ml. of 0.2 N HCl and 1086 ml. of distilled water.

APPENDIX B

DETERMINATION OF SHEAR STRESS

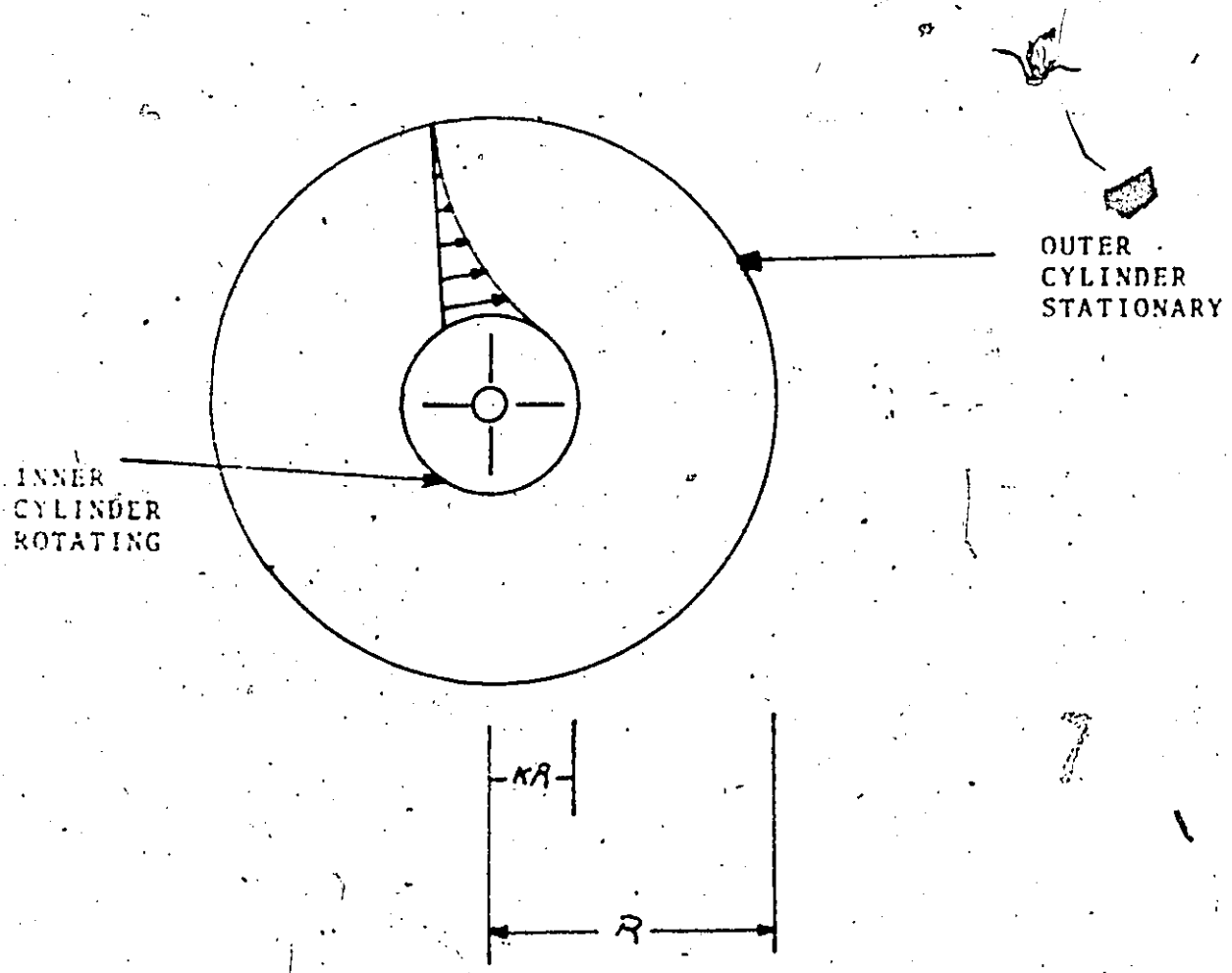

Figure B.1. Velocity Profile for Couette Flow with Rotating Inner Cylinder and Stationary Outer Cylinder.

For the case of steady state incompressible laminar flow, the fluid moves in concentric circles about the axis of the vertical cylinders and there are no velocity components in the vertical and longitudinal directions.

The equation of motion in the θ-direction may be written for the above case in cylindrical co-ordinates as

$$\frac{d}{dr}\left(\frac{1}{r}\frac{d(rv_\theta)}{dr}\right) = 0 \qquad (B.1)$$

with the following boundary conditions

$$v_\theta = 0 \quad \text{at} \quad r = r \qquad (B.2)$$

$$v_\theta = (KR)\,\Omega \quad \text{at} \quad r = KR \qquad (B.3)$$

where Ω is the angular velocity expressed in rad/sec.

Integrating Equation (B.1) twice with respect to r we obtain

$$v_\theta = \frac{c_1 r}{2} + \frac{c_2}{r} \qquad (B.4)$$

Now we solve for c_1, c_2 by using the boundary conditions to obtain

$$c_1 = \frac{-2\Omega K}{[-K+1/K]} \qquad (B.5)$$

$$c_2 = \frac{\Omega K R^2}{[-K+1/K]} \qquad (B.6)$$

Substituting into Equation (B.4) to obtain

$$v_\theta = \frac{\Omega R^2}{(1+1/K^2)}\left(\frac{r}{R^2} + \frac{1}{r}\right) \qquad (B.7)$$

The stress tensor for Newtonian fluids in cylindrical co-ordinates is given by (79).

$$\tau_{r\theta} = -\mu\left[r\frac{\partial}{\partial r}\left(\frac{v_\theta}{r}\right) + \frac{1}{r}\frac{\partial v_r}{\partial \theta}\right] \qquad (B.8)$$

but for Couette flow, $v_r = 0$ and

$$\tau_{r\theta} = -\mu\left[r\frac{\partial}{\partial r}\left(\frac{v_\theta}{r}\right)\right] \qquad (B.9)$$

Therefore, the shear rate,

$$\dot{\gamma} = r\frac{\partial}{\partial r}\left(\frac{v_\theta}{r}\right) \qquad (B.10)$$

$$\dot{\gamma}\Big|_{r=KR} = \frac{2\Omega}{K^2+1} \qquad (B.11)$$

For our experimental conditions

$$K^2 = .095$$

Therefore,

$$\dot{\gamma}\Big|_{r=KR} = \frac{2}{1.095}\,\Omega r \qquad (B.12)$$

or

$$\dot{\gamma}\Big|_{r=KR} = (1.82)(2\pi)(\text{RPM})/60 \qquad (B.13)$$

R.P.M.	$\dot{\gamma}$ (sec^{-1})
50	9.55
75	14.39
100	19.11
125	23.8
150	28.66
175	33.41
200	38.22

Table B.1. Conversion of R.P.M. to Shear Rate.

APPENDIX C

JUSTIFICATION FOR LINEAR LEAST SQUARES

The proposed model relating platelet diffusivity to shear rate and hematocrit is expressed mathematically as

$$D = H^{\beta} \dot{\gamma}^{n} \tag{C.1}$$

Equation (C.1) was transformed using logarithms to

$$\log D = n \log \dot{\gamma} + \beta \log H \tag{C.2}$$

And a linear regression was performed to obtain the best linear least square estimates of n and β.

This procedure is justified providing that the residuals associated with the transformation are normally distributed with mean zero and a constant variance. Referring to Figures C.1 and C.2 we see that this assumption is valid and therefore the use of linear least squares is justified.

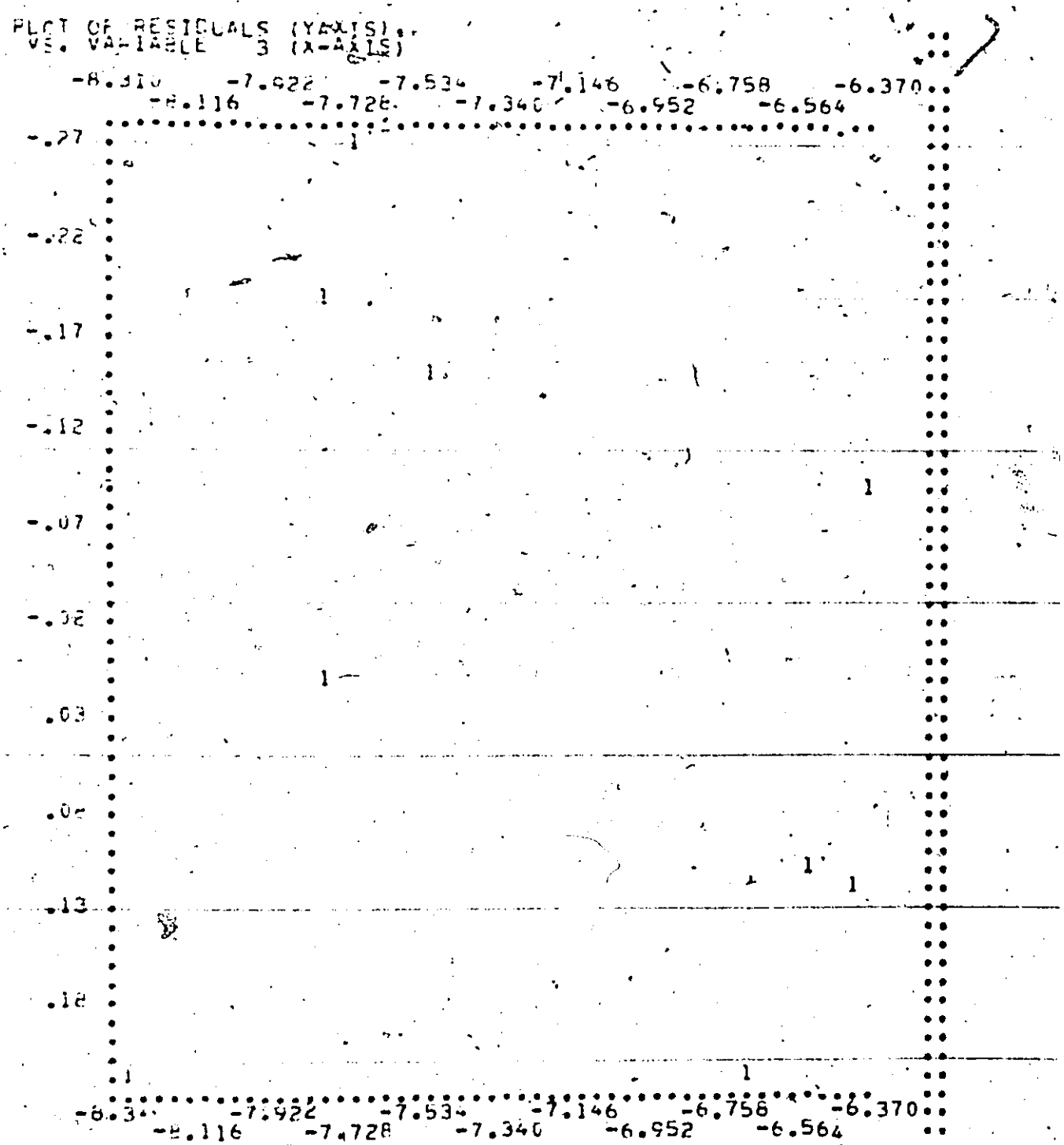

Figure C.1. Plot of Residuals against Platelet Diffusivity. The Data Used for this Regression is Plotted in Figure 5.2.3.

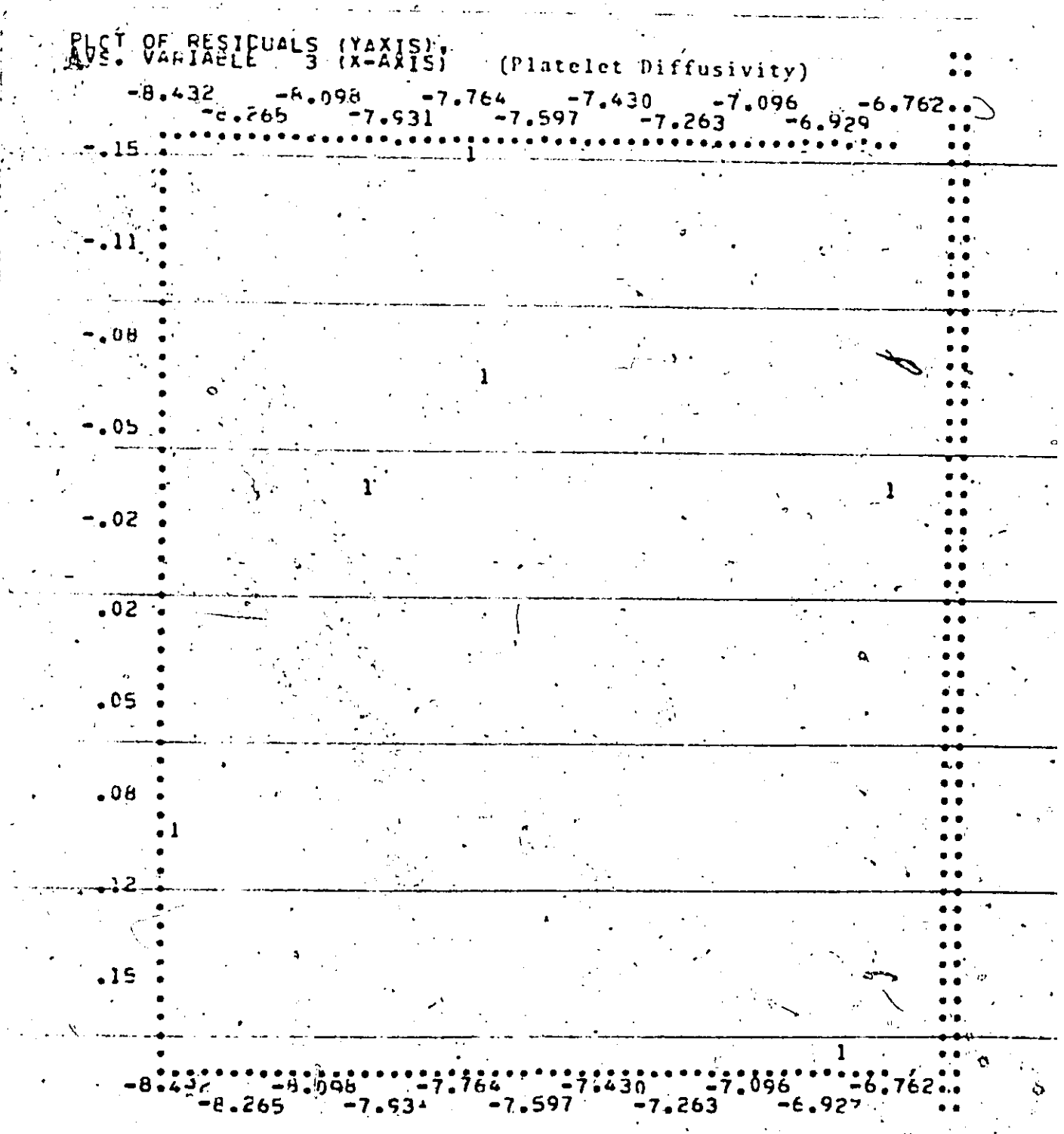

Figure C. 2: Plot of Residuals against Platelet Diffusivity. The Data Used for this Regression is Plotted in Figure 5.2.2.

APPENDIX D

AGGREGATION CURVE

Figure D.1 is the chart output from a standard aggregation test. The initial increase in the curve represents the increase in light transmission due to platelet aggregation. The later phase of the curve shows a gradual deaggregation of the platelets. This curve illustrates the viability of the platelets.

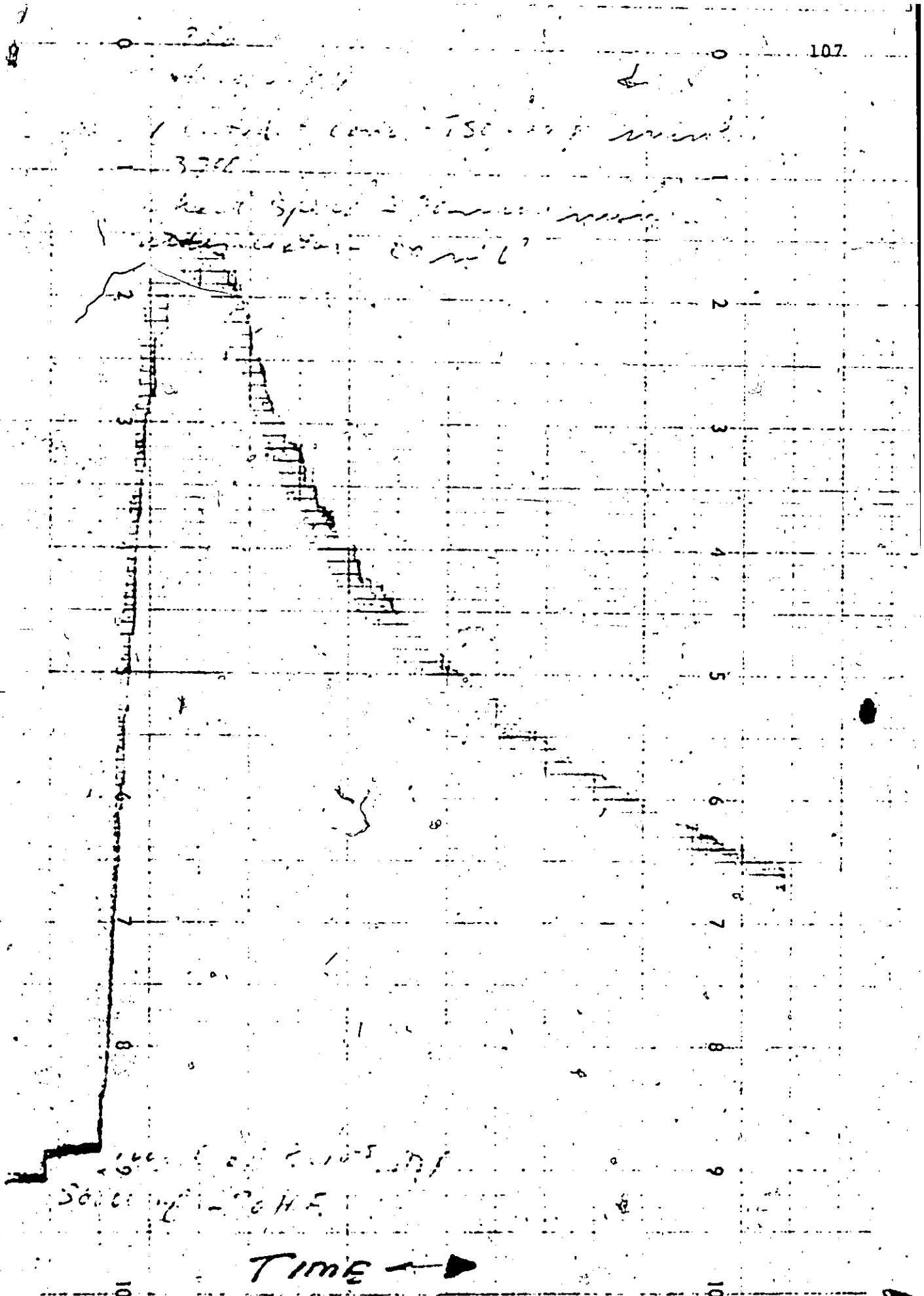

Figure D1. Platelet Aggregation Curve.